

Abstract

MICROBIAL CARBON ASSIMILATION WITHIN THE WALLS OF DEEP-SEA HYDROTHERMAL VENT CHIMNEYS

Heather N. Blumenfeld

June, 2011

Director: Dr. Matthew Schrenk

Department of Biology

Carbon is one of the most abundant elements on Earth stored in a multitude of reservoirs and constantly cycled through various processes occurring on our planet. Although it represents only a small percentage of the total carbon on Earth, the biosphere is the most active of all carbon reservoirs. We have a comparatively large knowledge of the surface biosphere and primary production associated with phytoplankton and green plants, as well as respiration of organic compounds. A substantial biosphere, driven by “dark energy” or chemical disequilibria may exist for kilometers beneath the continents and the seafloor. Water-rock reactions at high temperatures mobilize the reducing power of the deep Earth, and upon mixing with seawater produce copious and diverse energy sources which can support autotrophic growth. Several remarkable cases of chemotrophic carbon assimilation have been demonstrated since the discovery of the deep-sea vents more than 30 years ago (*e.g.* bacterial endosymbionts inhabiting the tube worm trophosome), and the isolation of a number of thermophilic and hyperthermophilic chemolithoautotrophs. To date, there are six known pathways of carbon assimilation, including the canonical Calvin Benson-Bassham pathway. All of the most recently discovered pathways have been found in thermophiles and Archaea specifically all likely to occurring at deep-sea hydrothermal vents.

This study seeks to document the occurrence of autotrophic microorganisms in the context of thermal and chemical gradients within the walls of deep-sea vent chimneys. Furthermore, we show that the phylogeny of genes associated with the Calvin Benson-Bassham cycle is associated with the environmental characteristics in which it occurs.

This work has implications for understanding feedbacks between environmental characteristics and carbon assimilation as well as the evolutionary history of carbon fixation pathways. These pathways were likely operative since early in Earth's history, and overlap with conditions which favor the abiotic synthesis of small organic molecules. Research in this realm thus may provide clues to the origins and diversification of carbon fixation pathways as well.

MICROBIAL CARBON ASSIMILATION WITHIN THE WALLS OF DEEP-SEA
HYDROTHERMAL VENT CHIMNEYS

A Thesis

Presented to

The Faculty of the Department of Biology

East Carolina University

In Partial Fulfillment

Of the Requirements for the Degree

Master of Science in Molecular Biology and Biotechnology

By

Heather N. Blumenfeld

June, 2011

© Heather Blumenfeld, 2011

MICROBIAL CARBON ASSIMILATION WITHIN THE WALLS OF DEEP-SEA
HYDROTHERMAL VENT CHIMNEYS

By

Heather N. Blumenfeld

Approved By:

Director of Thesis: _____

Matthew Schrenk, Ph.D.

Committee Member: _____

Baohong Zhang, Ph.D.

Committee Member: _____

John Stiller, Ph.D.

Committee Member: _____

Siddhartha Mitra, Ph.D.

Committee Member: _____

Cindy Putnam-Evans, Ph.D.

Chair of the Department of Biology: _____

Jeff McKinnon, Ph.D.

Dean of the Graduate School: _____

Paul J. Gemperline, Ph.D.

ACKNOWLEDGEMENTS

I want to start by thanking my thesis advisor, Dr. Matt Schrenk, for giving me an opportunity to work in his lab. During my last semester as an undergraduate student at ECU, I took microbiology by chance and developed a strong interest in the subject. I did research in the Schrenk lab to gain a sense of what microbiology research was like and then decided to pursue graduate study. I was on the fence about what I wanted to do when I graduated, and I was provided a great opportunity to grow as both a student and a scientist. Throughout my graduate career, I have been exposed to many new techniques and have had many great experiences that I will keep with me as I enter the professional world.

For specific contributions to my project, I would like to thank Dr. Deborah Kelley for providing me with sulfide chimneys for my study, Dr. Peter Girguis for giving me the opportunity to collaborate with Team Sulfide up at Harvard University, Dr. John Baross for contributing sequence data pertinent to my study, and Dr. Schrenk for the extensive community comparison he contributed to my thesis. I would also like to thank the Schrenk lab for all of their help and contributions to my project especially to Bridget Nelson, Billy Brazelton, and Amandeep Gujral for their technical support and expertise which helped in the completion of my thesis.

Some of the biggest thanks goes to my family, friends, and fiancé for all their support and encouragement throughout this process. They always provided an ear to listen when I had to vent, and a voice of reason during some of the most stressful times in my life. They are what helped motivate me and keep me going when times get tough and I am forever grateful to them.

Last, but not least, huge thanks goes out to my committee members: Dr. John Stiller, Dr. Baohong Zhang, Dr. Sidhartha Mitra, and Dr. Cindy Putnam-Evans for approving my project

and providing me with guidance and constructive criticism throughout the completion of my thesis.

This work was supported by the NASA Astrobiology Institute through the Carnegie Institution for Science and grants from the National Science Foundation.

TABLE OF CONTENTS

LIST OF TABLES	v
LIST OF FIGURES	vii
LIST OF ABBREVIATIONS	ix
CHAPTER I: INTRODUCTION	1
CHAPTER II: MICROBIOLOGY OF HYDROTHERMAL VENT CHIMNEYS FROM THE ENDEAVOUR SEGMENT, JUAN DE FUCA RIDGE	8
Introduction	8
What is a Chimney?	8
The Chimney Wall Environment	11
Methods used in Past Chimney Studies and Summary	13
Sampling Sites in this Study	15
Objectives	17
Hypotheses	18
Materials and Methods	19
DNA Extraction	19
16S rRNA Taxonomic Gene Assays	19
Real-time Quantitative Polymerase Chain Reaction	20
Terminal Restriction Fragment Length Polymorphism Analyses	22
Results	25
DNA Quantification	25
16S rRNA Taxonomic Screens	27

Archaea and Bacteria qPCR screens	28
t-RFLP analyses	31
Discussion	38
CHAPTER III: TAXONOMIC COMPARISON OF HYDROTHERMAL CHIMNEY	
MICROBIAL COMMUNITIES	41
Introduction	41
Objectives	44
Hypotheses	45
Materials and Methods	46
Compiling Clone Sequences	46
MOTHUR Community Analyses	46
Results	50
Discussion	58
Controls upon Microbial Community Composition in the Vent Chimney	
Habitat	58
Implication for Autotrophy and Microbial Community Structure	59
CHAPTER IV: ABUNDANCE AND DISTRIBUTION OF TYPE II CALVIN CYCLE GENES	
WITHIN VENT CHIMNEY MICROBIAL POPULATIONS	61
Introduction	61
The Global Carbon Cycle	61
Environmental Constraints	61
The Calvin-Bassham Cycle	62
Different Forms of RuBisCO	63

Evolutionary Significance	64
Objectives	66
Hypotheses	67
Materials and Methods	68
Total Organic Carbon Analyses	68
PCR Assay for the <i>cbbM</i> Gene	69
<i>cbbM</i> qPCR Analyses	71
Results	74
EA-IRMS	74
<i>cbbM</i> Gene Assays	75
<i>cbbM</i> qPCR Analyses	76
Discussion	79
CHAPTER V: PHYLOGENETIC ANALYSIS OF THE TYPE II CALVIN BENSON-	
BASSHAM PATHWAY FROM VENT CHIMNEYS	81
Introduction	81
Approaches to Study the Type II Calvin Cycle	81
Key Type II Calvin Cycle Participants	82
Evolutionary Significance of the Type II Calvin Cycle	83
Objectives	85
Hypotheses	86
Materials and Methods	87
Cloning <i>cbbM</i> Sequences and Exporting Files	87
Phylogenetic Analysis	89

Results	90
BLASTn	90
<i>cbbM</i> DNA Sequences	92
Protein Sequences	95
Discussion	97
CHAPTER VI: SUMMARY OF RESULTS	99
Introduction	99
Microbial Community Structure	99
Functional Diversity of Vent Chimney Inhabitants	104
Future Directions	107
REFERENCES	109

LIST OF TABLES

1.) Table 2-1: Cell abundance and diversity data from Finn	13
2.) Table 2-2: Primers used in taxonomic PCR assays	20
3.) Table 2-3: Primers used in taxonomic qPCR analysis	21
4.) Table 2-4: Primers Used in t-RFLP analysis	23
5.) Table 2-5: Restriction enzymes used in t-RFLP analysis	24
6.) Table 2-6: DNA Concentration Data	26
7.) Table 2-7: Results from 16S rRNA Assays for Bacteria and Archaea	27
8.) Table 2-8: Bacteria qPCR data	28
9.) Table 2-9: Archaea qPCR data	29
10.) Table 2-10: Archaea:Bacteria gene abundance ratios throughout chimney samples	30
11.) Table 2-11: Sample summary for bacteria t-RFLP analyses	31
12.) Table 2-12: Matrix generated through Bray-Curtis community similarity analysis for the <i>Hae</i> III digestion of Bacteria t-RFLP products	32
13.) Table 2-13: Matrix generated through Bray-Curtis community similarity analysis for the <i>Bst</i> I digestion of Bacteria t-RFLP products	34
14.) Table 2-14: Sample summary for Archaea t-RFLP analysis	35
15.) Table 2-15: Matrix generated through Bray-Curtis community similarity analysis for the <i>Rsa</i> I digestion of Archaea t-RFLP products	36
16.) Table 3-1: Microbial diversity studies of vent chimneys used in MOTHUR analyses	47
17.) Table 3-2: Microbial 16S rRNA sequence data incorporated into the study	49
18.) Table 3-3: Distribution of bacterial OTU's in composite analysis	51
19.) Table 3-4: Distribution of archaeal OTU's in composite analysis	56

20.) Table 4-1: Constraints on carbon assimilation pathways	62
21.) Table 4-2: Primers used in <i>cbbM</i> PCR assays	70
22.) Table 4-3: Primers used in <i>cbbM</i> qPCR assays	71
23.) Table 4-4: Key findings of <i>cbbM</i> gene assays	75
24.) Table 4-5: <i>cbbM</i> qPCR data	76
25.) Table 4-6: <i>cbbM</i> gene percentages among taxonomic gene abundances	77
26.) Table 5-1: <i>cbbM</i> positive samples cloned for phylogenetic analysis	87
27.) Table 5-2: Primers used in M13 PCR of cloned plasmid DNA	88
28.) Table 5-3: Top BLASTn matches to <i>cbbM</i> clone sequences in GenBank	91

LIST OF FIGURES

1.) Figure 2-1: Map of the Juan de Fuca Ridge	9
2.) Figure 2-2: Thermal and chemical gradients within a hydrothermal chimney wall	10
3.) Figure 2-3: Chimneys investigated in this study	15
4.) Figure 2-4: Standard curve from Archaea qPCR analyses	22
5.) Figure 2-5: Archaea and Bacteria qPCR summary chart	30
6.) Figure 2-6: Cluster diagram generated through Bray-Curtis community similarity analysis for the <i>Hae</i> III digestion of Bacteria t-RFLP products	33
7.) Figure 2-7: Cluster diagram generated through Bray-Curtis community similarity analysis for the <i>Bst</i> I digestion of Bacteria t-RFLP products	34
8.) Figure 2-8: Cluster diagram generated through Bray-Curtis community similarity analysis for the <i>Rsa</i> I digestion of Archaea t-RFLP products	36
9.) Figure 3-1: Map depicting locations of sampling sites used for the generation of clone libraries utilized in this study	48
10.) Figure 3-2: Cluster diagram showing the similarity of bacterial communities in different hydrothermal chimneys and in situ incubators using an OTU cutoff of 90% ...	50
11.) Figure 3-3: Cluster diagram showing the similarity of archaeal communities in different hydrothermal chimneys and in situ incubators using an OTU cutoff of 90% ...	54
12.) Figure 4-1: Gel image of a positive <i>cbbM</i> functional gene screen	70
13.) Figure 4-2: Standard curve used in <i>cbbM</i> qPCR gene quantification	72
14.) Figure 4-3: Melt curve at completion of <i>cbbM</i> qPCR run	73
15.) Figure 4-4: Results from EA-IRMS analysis of the sulfide chimney Finn	74
16.) Figure 4-5: Results summary from <i>cbbM</i> qPCR	77

17.) Figure 5-1: Simplified complete neighbor-joining phylogenetic tree of <i>cbbM</i> DNA sequences	92
18.) Figure 5-2: The detailed upper branch of the phylogenetic tree of <i>cbbM</i> DNA sequences	93
19.) Figure 5-3: The bottom-branch, “Mothra Vent Chimney” community, DNA sequence cluster from the Finn chimney ecosystem	95
20.) Figure 5-4: Simplified complete neighbor-joining phylogenetic tree of <i>cbbM</i> protein sequences	96
21.) Figure 6-1: Model for vent evolution and subsequent microbial colonization	103
22.) Figure 6-2: <i>cbbM</i> distribution amongst chimney habitats	106

LIST OF ABBREVIATIONS

Ma: Megaannum, million years

DOM: Dissolved Organic Matter

DOC: Dissolved Organic Carbon

CBB: Calvin Benson-Bassham

rTCA: Reverse Tricarboxylic Acid Cycle

Acetyl-CoA: Reductive Acetyl-Coenzyme A Pathway

RUBP: Ribulose-1, 5-bisphosphate

RuBisCO: Ribulose-1,5-bisphosphate carboxylase oxygenase

GT: gigaton

JdFR: Juan de Fuca Ridge

MGI Cren: Marine Group I Crenarchaeota

DHVE: Deep-sea hydrothermal vent euryarchaeal group

HWCG: Crenarchaeota subgroup

ND: not determined

Ext: Exterior chimney gradient

Mid: Middle chimney gradient

Int: Interior chimney gradient

Inc: Incubator

Adj: Adjacent

Bkdg: Background

SW: Seawater

HF: Hydrothermal Fluids

ES: Endeavour Segment

TOC: total organic carbon

MEF: Main Endeavour Field

DNA: Deoxyribonucleic acid

PCR: Polymerase chain reaction

rRNA: ribosomal ribonucleic acid

Arch: Archaea

Bac: Bacteria

qPCR: Quantitative Polymerase Chain Reaction

BP: Base pair

S&M: Smoke and Mirrors sulfide chimney

t-RFLP: terminal restriction fragment length polymorphism

OTU's: Operational Taxonomic Units

SMT: Southern Mariana Trough

EPR: East Pacific Rise

Seqs: Sequences

ATP: adenosine triphosphate

EA-IRMS: Elemental Analysis – Isotope Ratio Mass Spectrometry

LB: Luria Broth

AMP: Ampicillin

ACN: Accession

Med: Mediterranean

Uncul: Uncultured

Sed: Sediment

Tube: Tubeworm

Proteo: Proteobacteria

CHAPTER I: INTRODUCTION

Hydrothermal fluid circulation is pervasive throughout the shallow sub-seafloor driven by magmatic upwelling or by cooling rocks from deep within the Earth's interior. At the mid-ocean ridges, buoyant "end member" hydrothermal fluids consisting of dissolved minerals and volatile compounds are emitted into the deep-sea. The mixing of hot, reducing, metal-rich, hydrothermal fluids (>300°C) with cold, oxygenated seawater (2°C) results in the precipitation of sulfide minerals and the formation of steep-sided structures known as "black smoker" chimneys. Black smokers are permeable and porous conduits for hydrothermal fluids that host a diverse assemblage of macro and micro-fauna. A much larger habitat is sustained within the ridge flank hydrothermal environment. Ridge flank hydrothermal circulation represents a major mechanism of biogeochemical exchange between the deep ocean and the subsurface, and extends to at least 65 Ma away from the mid-ocean ridge axes, covering a major swath of the global seafloor. Vent chimneys are a high temperature environment which can provide a "window" to processes happening deep within the Earth's crust (Deming and Baross 1993). These systems also provide an avenue for biologists to study the limits to life on Earth and the constraints hydrothermal systems place upon biological processes (Schrenk, Holden et al. 2008).

It was speculated since the discovery of the deep-sea vents in the late 1970's that volcanically-fueled autotrophic microbial growth could represent a major source of primary production in the deep-sea (Jannasch 1985), and that this could occur potentially decoupled from processes at the Earth's surface. Follow-up studies have calculated the substantial free energy yields that can be harnessed to support chemolithoautotrophic microbial growth based upon chemical disequilibria from fluid mixing (McCollom and Shock, 1997; McCollom, 2000; Amend and Shock, 2001). The most prevalent source of energy in hydrothermal environments comes

from sulfur oxidation, but other energy sources can be used such as sulfate, iron, and hydrogen (McCollom and Shock 1997). Despite the enrichment and isolation of numerous autotrophic microorganisms from hydrothermal vent environments in subsequent years, few studies have shown that this process is occurring *in situ* at appreciable rates (although this situation is changing to some extent in the post-genomics era) (Eberhard, Wirsen et al. 1995).

Complementary to the microbiological studies, major advancements have also been made in understanding organic carbon transformations during fluid flow through the hydrothermal vent subsurface. Although few studies have generated quantitative data on organic geochemistry, it is recognized that organic carbon content varies between hydrothermal chimneys and is linked to the aging process from nascent chimneys to more mature chimneys colonized by macrofauna. Studies of dissolved organic matter (DOM) and particulate in circulating hydrothermal fluids have shown that a higher organic carbon content ($49 \pm 9 \mu\text{M}$) is found within low temperature, diffuse flow vents while lower organic carbon content ($15 \pm 5 \mu\text{M}$) is specific to off-axis, high temperature vents (Lang, Butterfield et al. 2006). This is coincident with the amount of chemical energy available for biosynthetic processes. In diffuse-flow systems there is higher productivity demonstrated by increased cell counts, methane production, nitrate reduction, and sulfide oxidation. This leads to the thought that autotrophy may be the sole source of dissolved organic carbon (DOC) in these environments (Lang, Butterfield et al. 2006). It is also thought that hydrothermal circulation provides a huge carbon sink which is bio-processed through microbial autotrophy and distributed to underlying oceanic crust. This is seen through characteristic isotopic and fractionation patterns associated with autotrophic processes. These values differ between old and new oceanic crust leading to the conclusion that over time microbial communities fix carbon through diverse metabolic processes (McCarthy, Beaupre et al. 2011).

Chemolithoautotrophy driving the biological assimilation of inorganic carbon sources is thought to be the primary microbial metabolism in younger portions of hydrothermal ecosystems due to relatively low availability of fixed organic carbon. In recent years, the magnitude and extent of a subsurface biosphere, subsistent upon chemical energy rather than light has become widely recognized (Bach, Edwards et al. 2006). Autotrophy in environments removed from the photic zone, such as in deep oceanic environments, has not been well characterized, but may prove to be a potential unidentified sink for atmospheric carbon dioxide. Organisms in these systems are dependent upon energy in the form of chemical disequilibria to drive their metabolisms. Many chemolithoautotrophs (which fix carbon by using chemical energy) have been cultured. Chemolithoautotrophy occurs through multiple pathways including the Calvin Benson-Bassham (CBB) Cycle, the Reverse Tricarboxylic Acid Cycle (rTCA), and the Reductive Acetyl CoA (Acetyl CoA) pathway among others. The Calvin Cycle is the only carbon-fixation pathway that occurs in both the photic and non-photoc zones and is the main focus of experiments in this study. The majority of the other pathways are carried out by thermophilic bacteria and Archaea that reside in and around high temperature habitats (Hugler, Huber et al. 2003).

The CBB cycle is the most predominant carbon fixation pathway on modern day Earth, at least in near surface environments. This pathway is used by organisms in the biosynthesis of carbohydrates. Carbon dioxide (CO_2) is fixed through the carbon acceptor ribulose-1, 5-bisphosphate (RUBP) with the aid of the enzyme ribulose-1, 5-bisphosphate carboxylase oxygenase (RuBisCO). RuBisCO serves as the key regulatory enzyme within the CBB cycle. There are at least four different forms of RuBisCO adapted to specific environments and contained within different organisms. In hydrothermal ecosystems, it has been found that,

organisms use Form II RuBisCO in their CBB cycle (Nakagawa and Takai 2008). This form of RuBisCO is coded by the *cbbM* gene. The presence and distribution of this gene among microbial communities is one of the main focuses of this study.

Additional autotrophic pathways may contribute to carbon assimilation in the hydrothermal vent ecosystem, but were not analyzed in the current study, including the rTCA pathway and the Acetyl CoA pathway amongst others. The rTCA pathway is thought to be operative in deep sea hydrothermal environments with organisms inhabiting reducing transition zones between hot hydrothermal vents and low temperature zones surrounding them. Main participants in the pathway are anaerobes and microaerophiles due to this pathway's oxygen-sensitive enzymes (Berg, Kockelkorn et al. 2010). The reductive acetyl CoA pathway is thought to be the first carbon fixation pathway to exist. This is due to the fact that all enzymes in this pathway are oxygen-intolerant which corresponds to early Earth conditions (Thauer 2007). This pathway requires the least energy to operate but is costly in the respect for its demand of metals, cofactors, and low reducing substrates (Berg, Kockelkorn et al. 2010). This pathway is strictly anaerobic containing key regulatory enzymes with high oxygen sensitivity and is operative in methanogenic *Archaea* in hydrothermal chimney environments (Nakagawa and Takai 2008).

Even though these pathways have all been shown to be present in hydrothermal systems, there are a set of environmental and physical constraints controlling which pathways are utilized. As mentioned previously, presence or absence of oxygen places a selective pressure upon the operation of specific pathways confining them to chimney gradients with optimal oxygen conditions. In addition, high energetic costs are associated with synthesizing autotrophic catalysts and enzymes. This is dependent on the amount of useable energy available, placing a

hold on what pathways are used. Most importantly, the amount of CO₂ available for assimilation plays a factor on how much biosynthesis takes place. With a large quantity of bicarbonate dissolved within the ocean environment, organisms that acquire abilities to use this carbon form in their autotrophic pathways are at an advantage (Berg, Kockelkorn et al. 2010).

Currently there is proof that there are six autotrophic carbon fixation pathways. Due to the vast diversity of pathways, but central carbon fixation methods it leads one to believe they may be tied together evolutionarily. The advent of these pathways is thought to stem from coping with the extreme environment of early Earth conditions. Through the study of autotrophic pathways found within hydrothermal environments, the evolution of carbon assimilation into biological systems on Earth can be further understood (Berg, Kockelkorn et al. 2010).

It is important to study carbon assimilation in hydrothermal environments because it is thought that the largest reservoir of dissolved organic carbon is found within the deep ocean environment (~680 GT), similar to the amount of CO₂ found within the atmosphere (Lang, Butterfield et al. 2006). It has been shown that at ridge-flank hydrothermal systems, containing little dissolved organic carbon, there is a large amount of organic crustal removal by either microbial activity or through biosynthesis over the course of 10,000 year crustal residence (McCarthy, Beaupre et al. 2011). Developing tools to understand organic carbon cycling in deep sea hydrothermal systems can aid towards understanding its role the global carbon cycle.

Through the study of autotrophy in hydrothermal systems, clues can be determined into how life originated on our planet. Mineral-catalyzed reactions aid in the conversion of inorganic carbon to small organic compounds which are common under hydrothermal vent conditions (Cody, Boctor et al. 2004). Reaction surfaces within hydrothermal environments resemble iron-sulfur enzymes and cofactors operative in autotrophic pathways. This leads to the theory that life

originated within hydrothermal environments through mineral-catalyzed reactions allowing for self-replication and the self-assembly of early biomolecules (Berg, Kockelkorn et al. 2010).

Autotrophic pathways are presumed to be deeply-rooted in the evolutionary history of organisms on our planet. In addition to the oxygen sensitive autotrophic pathways hydrothermal conditions have been speculated to be conducive to lateral gene transfer may have helped pass carbon fixation genes along to many organisms. It has been shown that transposases are present in high abundance in hydrothermal systems facilitating lateral gene transfer amongst microorganisms (Brazelton and Baross 2009). The existence and potential use of multiple pathways in these ecosystems could be evidence of these occurrences. Through the elucidation of these pathways in organisms throughout hydrothermal systems, clues to the development of some of the earliest forms of life can be discovered (Thauer 2007).

The specific contribution made in this study was to further examine the CBB cycle in hydrothermal chimney environments in particular. Most studies on the CBB cycle within hydrothermal environments have been performed on microbial *Gammaproteobacteria* endosymbionts living on or around hydrothermal vents (Nakagawa and Takai 2008). There have only been a handful of systematic approaches used to identify the presence of the CBB cycle throughout chimneys themselves. Experiments in this study were aimed at 1.) characterizing the microbial composition of hydrothermal ecosystems through the examination of key microbial assemblages and taxonomic groups found within different chimney gradients. 2.) Downstream analyses aimed at linking microbial diversity to functional diversity through pinpointing the presence of the *cbbM* gene within the microbial populations. Therefore, to provide a broader picture of CBB cycle activity, the microbial population in this study encompassing multiple chimneys and gradients was screened for *cbbM*. Complementary to these results, gene abundance

data was compiled to show how much of the bacteria and Archaea population are comprised of potential CBB cycle participants. Finally, the distribution of *cbbM* genes was examined amongst two different chimney populations using phylogenetic analyses. Through this study, the occurrence and diversity of the *cbbM* gene within the microbial chimney environment was further investigated. Results from this study will provide an important contribution to data on the Type II Calvin Benson-Bassham cycle within hydrothermal chimney ecosystems and provide clues as to the environmental and evolutionary controls upon the utilization of this important carbon fixation pathway.

CHAPTER II: MICROBIOLOGY OF HYDROTHERMAL VENT CHIMNEYS FROM THE
ENDEAVOUR SEGMENT, JUAN DE FUCA RIDGE

INTRODUCTION

What is a Vent Chimney?

Hydrothermal vent chimneys come in a range of forms. Their morphology is influenced by factors including how vigorous the hydrothermal venting is, the chemistry of the vent fluids and host rocks, and the tectonic activity in the region. At the intermediate-spreading Juan de Fuca Ridge (JdFR) in the northeast Pacific Ocean (Figure 2-1), black smoker chimneys are tall, steep structures, reaching up to 45 m in height, likely due to their cementation with amorphous silica.

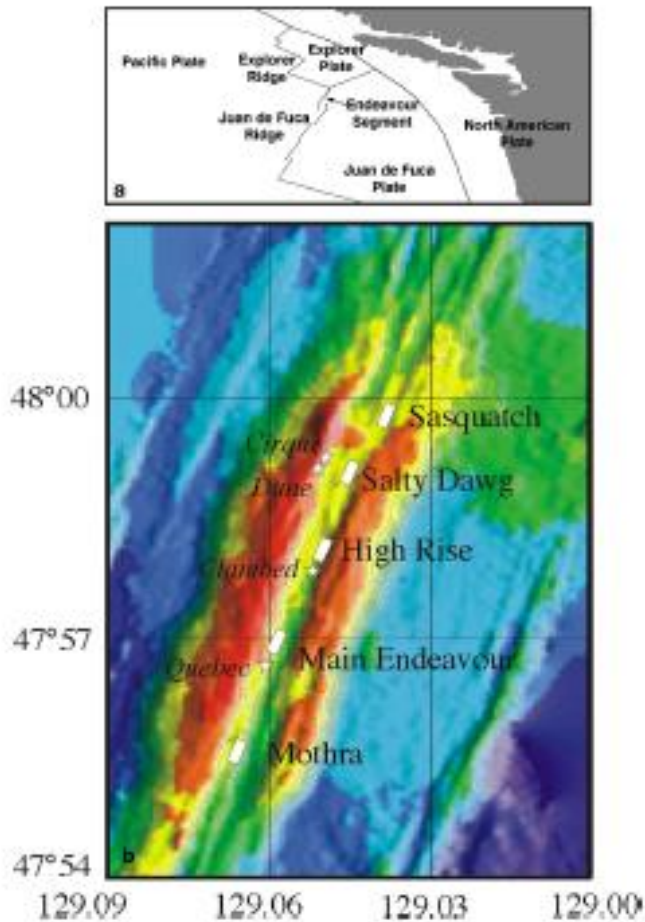
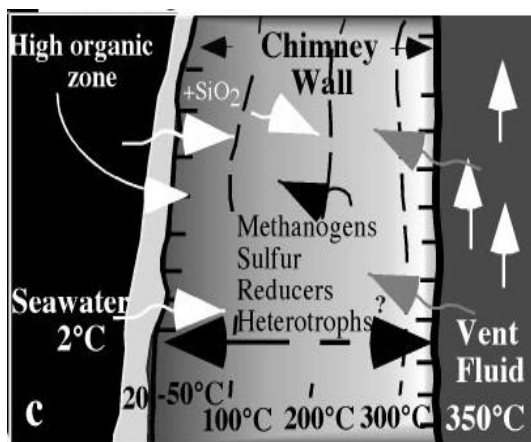
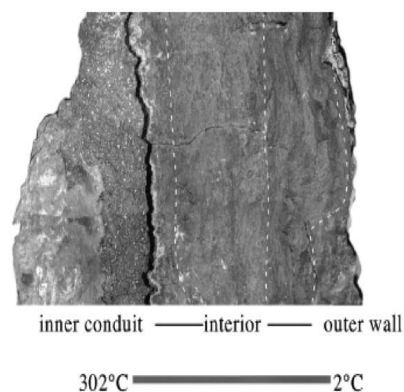


Figure 2-1: Map of the Juan de Fuca Ridge (Kristall, Kelley et al. 2006)

Within the walls of hydrothermal chimneys, spanning anywhere from a few cm's to a meter in thickness, there are intense thermal and chemical gradients resulting from the large contrast in temperature from the chimney's interior to exterior regions. Hydrothermal fluids arise through the central conduit of the chimney which is in direct contact with the internal wall of the chimney. The exterior wall of the chimney is in direct contact with seawater (Schrenk, Holden et al. 2008). A depiction of the thermal and chemical gradients present in hydrothermal vent chimneys is shown below in Figure 2-2.



2-2A.



2-2B.

Figure 2-2: Thermal and chemical gradients within a hydrothermal chimney wall. 2-2A: Thermal-chemical gradients across a typical black smoker chimney wall (Kelley, Baross et al. 2002); 2-2B: Mineralogy and structure of a black smoker chimney wall, *Finn*, from the Mothra Vent Field, Endeavour Segment, Juan de Fuca Ridge (Schrenk, Holden et al. 2008).

Within chimney walls there are distinct gradients which host diverse communities of microorganisms. The establishment of gradients within hydrothermal chimneys is influenced through fluid mixing, porosity, mineralogy, and fluid chemistry. Chimney exterior gradients, in direct contact with seawater, have 12-36% porosity allowing the circulation of low temperature seawater (Kelley, Baross et al. 2002). Exterior gradients' surfaces are host to macrofaunal communities with temperatures ranging from 2-30°C. These gradients have very similar fluid chemistry to oxygenated seawater providing habitats for aerobic psychrophilic to mesophilic microbial communities (Schrenk, Kelley et al. 2003). Sulfur oxidation serves as the main energy source for microbial metabolisms observed through the abundance of oxidized sulfur minerals throughout exterior gradient mineralogy (McCollom and Shock 1997; Schrenk, Kelley et al. 2003). Middle chimney gradients, known as diffuse mixing zones, have intermediate fluid mixing between hot hydrothermal fluids and cold seawater generating fluid temperatures ranging

from 30-50°C (McCollom and Shock 1997). The mineralogy of these environments is categorized by silified pyrite and zinc sulfide (Schrenk, Kelley et al. 2003). Fluids are slightly more reducing in nature allowing sulfate and sulfur reduction to drive chemosynthesis. These gradients act as transition zones between aerobic and anaerobic environments throughout the chimney wall (Kelley, Baross et al. 2002). Interior gradients, nearest to the chimney's central conduit, have overall higher temperatures due to vigorous mixing hot hydrothermal fluids with rare seawater intrusions (McCollom and Shock 1997). Temperatures can reach up to 150°C due to episodic emissions of hydrothermal fluids (>300°C) from the central conduit. These gradients are composed of porous pyrite and zinc sulfide with chalcopyrite and anhydrite lined fissures from the previously-mentioned hydrothermal fluid emissions (Schrenk, Kelley et al. 2003). A highly reducing environment in interior chimney gradients facilitate methotrophy and methanogenesis-driven metabolisms.

The Chimney Wall Environment

During hydrothermal venting, fluid mixing sustains chemical disequilibrium between the vent fluids and seawater which supports a range of chemical reactions which produce free energy and can be catalyzed by biology (Amend and Shock 2001). These catabolic processes can be harnessed by microorganisms to drive biosynthesis (anabolism); the energy sources for catabolism can be either organic or inorganic. Organisms that use chemical energy coupled to the conversion of inorganic carbon to biomass are known as chemoautotrophs. Autotrophic mechanisms have been shown to occur in hydrothermal systems through a number of geochemical and microbiological studies such as the isolation and characterization of organisms, and stable isotope analysis at a range of different trophic levels. These have shown that chemical disequilibrium provides viable energy sources to drive these metabolisms (Amend and Shock

2001), and the favored processes vary depending upon temperature and the extent of mixing between hydrothermal fluids and seawater. The extent and characteristics of microorganisms found throughout different regions of hydrothermal chimneys is believed to be determined by temperature, oxygen availability and the amount of organic and inorganic materials available for biosynthesis. Temperature places a first order constraint on life with limits ranging from 2°C-122°C. Thermal-chemical models have demonstrated that different types of metabolisms are adapted to specific locations within the mixing gradients. Aerobic metabolisms are found at lower temperatures while anaerobic metabolisms are specific to higher temperatures (Schrenk, Holden et al. 2008).

Early “nascent” vents are presumed to be largely colonized by autotrophs, but as they solidify and develop, more heterotrophs and tube worms with their associated communities move in. With time, the tube worms and exterior biomass becomes encased within the growing chimney structure (Schrenk, Kelley et al. 2003; McCliment, Voglesonger et al. 2006). Ongoing studies seek to refine models of chimney growth and development and the conditions related to specific “zones” interior to chimney walls (Tivey, Humphris et al. 1995). One approach has been to integrate instruments into the growing chimney structure. These instruments typically contain an array of thermocouple probes and in some case chemical sensors. In many cases these instruments contain colonization experiments (or “incubators”), aimed at promoting microbial growth within the chimney environment. To date, most of the substrata that have been emplaced within growing chimney walls have been inorganic and inert, and therefore provide an analog to organic-poor chimney materials during the early stages of chimney growth (Reysenbach, Longnecker et al. 2000; McCliment, Voglesonger et al. 2006).

Methods used in Past Chimney Studies and Summary

Due to their remote location, and specialized equipment required, microbiological studies of hydrothermal vents have been very limited. Most of what is known is based off molecular-based characterization of organisms and identifying biomolecular signatures, and to a lesser extent through cell cultures (Schrenk, Holden et al. 2008). The culmination of studies and knowledge provide a summary of what is known about these systems, but to this date there has not been a full systematic, biogeographical study characterizing these systems.

Previous phylogenetic and cellular abundance studies aimed towards the microbial characterization of the black smoker Finn, one of the many black smokers found along the JdFR. Results were collected during an active venting period with 302°C hydrothermal fluid temperatures. The results of this study are summarized below in Table 2-1.

Table 2-1: Cell abundance and diversity data from Finn (Schrenk, Kelley et al. 2003)

Sample Type	T (°C)	Size	Gradient	Cells (g-1)	Archaea	Bacteria
Very Large	302	12-20 cm	ext.	1.90E+06	MGI Cren.	<i>γ,ε-proteobacteria</i>
Chimney Wall					DHVE	
(Finn)			mid-ext.	1.70E+08	<i>Thermococcales</i>	
					MGI Cren.	
					<i>Archaeoglobales</i>	
			mid-int.	1.90E+07	HWCG (Cren.)	
			int.	2.10E+05	ND	

Upon interpretation of cellular abundance data, it can be seen that the amount of biomass varies throughout the length of the hydrothermal chimney wall indicating higher cell densities found towards outer regions of the chimney, with especially high biomass in the middle zones. Middle regions of the chimney wall are believed to experience high diversity due to their location directly between the cold seawater (SW) and hot hydrothermal fluid (HF) barriers. Upon interpretation of the complementary phylogenetic data, there also appears to be a transition from

Bacteria to Archaea from outer to inner regions of the chimney wall. Throughout the length of the chimney wall, Archaea species vary. Exterior Archaea species most resemble common deep sea organisms, middle gradient possess the most microbial diversity, and interior gradient species resemble organisms found in the deep subsurface and high temperature regions (Schrenk, Holden et al. 2008).

Additional hydrothermal microbiology studies (Schrenk, Holden et al. 2008) have shown similar results, but there is some variation between the microbial compositions between sites. In addition, sampling methodology has varied study-to-study leading to difficult site characterization and comparison. Even though investigation has proved difficult there were some conclusions made through the compilation of these studies. Studies have shown that there are higher cellular abundances and DNA concentrations found towards the middle and exterior portions of hydrothermal chimney walls (Schrenk, Kelley et al. 2003). In addition, some conclusions can be made about microbial colonization of younger versus older chimneys. It has been shown that younger chimneys with low total organic carbon (TOC) content are colonized mostly by autotrophs, but over time as more organic carbon is produced by autotrophs, heterotroph colonization occurs (Takai, Komatsu et al. 2001; Schrenk, Kelley et al. 2003). This leads to the conclusion that the amount of TOC present in hydrothermal systems is related to the microbial composition of the system.

This study seeks to verify that these trends occur within the chimney materials that are the basis of this thesis using a combination of DNA extraction and quantification, PCR and quantitative PCR analyses, and terminal restriction length polymorphism analysis.

Sampling Sites in this Study

Chimney structures for this study were collected from the Endeavour Segment (ES) of the JdFR, located in the northeastern Pacific Ocean, approximately 300 km off the coast of Washington State. The ES is one of the most well studied hydrothermal spreading centers and contains both high temperature ($>350^{\circ}\text{C}$) and low temperature vents ($<100^{\circ}\text{C}$). The ES hosts five individual vent fields, space 2-3 km apart with slight variations in vent temperature and fluid chemistry (Kelley, Delaney et al. 2001). Different chimneys were investigated in this study found throughout the Juan de Fuca Ridge system including Finn, and Roane from the Mothra vent field, and Hulk (not pictured) from the Main Endeavour Field (MEF) (Figure 2-3).

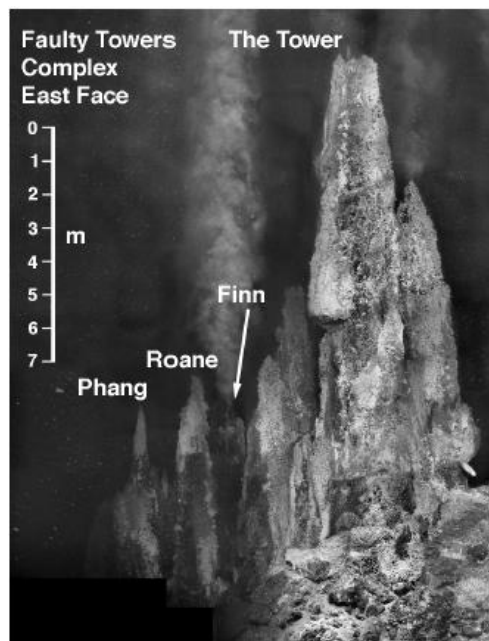


Figure 2-3: Chimneys investigated in this study: Finn and Roane (Kristall, Kelley et al. 2006).

The majority of analyses were conducted on the black smoker *Finn*. Finn contains an open central conduit that actively vents fluids reaching temperatures around 302°C . The central conduit is surrounded by walls 5-32 cm thick which are surrounded by seawater with temperatures ranging between $2\text{-}10^{\circ}\text{C}$. The contrast in temperature from the interior to exterior

portions have gradients ranging up to 300°C allowing for diverse ecological niches for microorganisms residing within this ecosystem. In addition to thermal variability, there are diverse physical and chemical conditions extending throughout the breadth of the chimney. Differences in mineral content, porosity, and fluid mixing allow for diverse ecosystems throughout the chimney structure (Schrenk, Kelley et al. 2003).

Roane lacks an open central conduit, but is composed of numerous channels and pore spaces that enclose a conduit that actively vents fluids around 280°C. Roane is a diffuse flow system with four defined zones: a fossil worm tube zone, a silica zone, and an outer and inner sulfide zone. This system contains exterior macrofaunal growth and interior pore spaces providing environments for microfauna (Kristall, Kelley et al. 2006).

Hulk is one of the many large chimney structures found within the Main Endeavour Field also located on the JdFR. This chimney actively vents fluids around 316°C. Chimneys within the Main Endeavour Field have a high Archaea population with up to 65% of interior regions being composed of Archaea. Phylogenetic studies have shown the majority of chimney inhabitants are Archaea in the form of Crenarchaeota (Ver Eecke, Kelley et al. 2009).

OBJECTIVES

To provide a basis for functional interpretations of the deep-sea hydrothermal chimney ecosystem, data related to microbial abundance and community composition is necessary. The nature of this project deals with three different chimneys within two different hydrothermal vent fields. In order to start doing analyses one needs to classify what sources of carbon are available for organisms to utilize and how much biomass is present within the system. In addition, comparative microbial community diversity analyses must be conducted to identify the uniqueness of each system. Together these analyses will provide data pertinent to the project and will help in result interpretation. Thus, the main objectives of this chapter are:

- 1.) Characterizing microbial environmental characteristics in terms of overall biomass (DNA concentrations) throughout chimney gradients.
- 2.) Providing a baseline of the taxonomic composition of samples for this study through the screening of samples for both Archaea and Bacteria species.
- 3.) Conducting archaeal and bacterial quantitative polymerase chain reaction (qPCR) analyses to determine the relative abundances of Archaea and Bacteria throughout chimneys studied.
- 4.) Using bacterial and archaeal terminal restriction fragment length polymorphism (t-RFLP) analysis to look at diversity throughout chimney communities.

HYPOTHESES

The following hypotheses will be tested in this chapter: 1.) Higher biomass is found in mid-exterior zones of chimney walls.

2.) Archaeal sequences are more abundant than bacteria in interior regions of the chimney wall.

3.) Microbial community diversity varies dependent on specific environmental conditions.

4.) The highest species richness is found in mid-exterior zones.

MATERIALS AND METHODS

Experiments in this study were conducted in order to help characterize the microbiology of hydrothermal environments. The determination of microbial biomass and community compositions allows one to gain an overall means to compare and characterize these ecosystems.

DNA Extraction

DNA extraction was performed using a method developed by Edwards et al. in 2000 (Edwards, Bond et al. 2000). Due to low extraction yields, extractions were purified (QiaQuick PCR Purification Kit, QIAGEN) and pooled in order to obtain sufficient quantities for further analyses. DNA was quantified using either a Qubit fluorometer (Invitrogen) or Nanodrop 2000 (ThermoScientific).

16S rRNA Taxonomic Gene Assays

Genomic DNA extracted from sediments and chimney rocks was first screened for taxonomic (16S) ribosomal ribonucleic acid (rRNA) genes to document whether archaeal or bacterial species predominated. The 16S (small subunit) of rRNA is found within all cells since all cells contain ribosomes; therefore, this gene is used to determine evolutionary relationships between organisms. This gene has highly conserved and hyper-variable regions which allow for many genomic applications (Madigan and Martinko 2006). Through both bacterial and archaeal screens, a highly conserved region was amplified using the universal B27F/1492R and 21F/958R primer sets respectively. These primer sets amplified a 1500 base pair (BP) segment of the bacterial 16S rRNA gene and a 1600 BP segment of the 16S rRNA gene. Primers sets used in these studies are shown below in Table 2-2.

Table 2-2: Primers used in taxonomic PCR assays (Weisburg, Barnes et al. 1991; Delong 1992)

Primers	Gene Target	Primer Sequence (5'-3')	BP	Cycling Conditions
<i>Bacteria</i>				
B27F	Bacteria 16s rRNA	AGAGTTTGATCCTGGCTCAG	1500	94°C 2 min; 40 cycles: 94°C 30 sec, 54°C
1492R		GGTACCTTGTTACGACTT		45 sec, 72°C 2 min; 72°C 10 min
<i>Archaea</i>				
21F	Archaea 16s rRNA	TTCCGGTTGATCCYGCCGGA	1600	94°C 5 min; 40 cycles: 94°C 30 sec, 55°C
958R		YCCGGCGTTGAMTCCAATT		45 sec, 72°C 2 min; 72°C 6 min.

Each 20 µl PCR reaction contained: 1 µl of template, 1× buffer, 0.2 mM dNTPs, 0.25 µM forward and reverse primers respective to analysis, 1 U *Taq* polymerase, and molecular-grade water to make up the total volume of reaction. Results from PCR reactions were visualized on 1% agarose gels run at 95V.

Real-time Quantitative Polymerase Chain Reaction (qPCR):

To gain a sense of the overall abundance of key taxonomic genes in both bacteria and Archaea, qPCR was performed. qPCR provides a fast and quantitative approach to measuring relative gene abundances within environmental samples (Fierer, Jackson et al. 2005). Assays were conducted using a CFX96 Real-Time PCR Detection System (Bio-Rad) utilizing a SYBRgreen fluorescent probe in the Ssofast Evogreen mix (Bio-Rad) to measure the amount of gene copies generated throughout the course of 40 PCR cycles. The primers and respective cycling conditions used for both Bacteria and Archaea qPCR amplification are shown below in Table 2-3.

Table 2-3: Primers used in taxonomic qPCR analysis (Fierer, Jackson et al. 2005)

Primers	Gene Target	Sequence (5'-3')	Size (BP)	Cycling Conditions
EUB 338	Bac 16s rRNA	ACTCCTACGGGAGGCAGCAG	200	98°C 2 m; 40 cycles:
EUB 518		ATTACCGCGGCTGCTGG		98°C 2 s, 60°C 2 s
A958F	Arch 16s rRNA	AATTGGABTCAACGCCGGR	95	98°C 2 m; 40 cycles:
1048arcR		major-CGRCGGCCATGCACCWC		98°C 2 s, 59.7°C 2 s
		minor-CGRCRGCCATGYACCWC		

Assays were run in triplicate with each 20 µl reaction containing: 1 µl template DNA (either full strength or 0.1 dilutions), 10 µl Ssofast Evagreen mastermix, 0.5 µM forwards and reverse primers, and molecular-grade water to make up the final volume of the reaction mixture.

Quantification was made through use of diluted pure culture DNA standards: *Escherichia coli* for bacteria, and *Methanocaldococcus jannaschii* for Archaea. Standards were run in triplicate with limits of detection ranging from 137 – 4.37E6 16S gene copies/ g sample (0.02 pg/µl– 0.64 ng/µl) for bacteria assays and 105-3.37E8 16S gene copies/ g sample (0.02 – 64 ng/µl) for Archaea assays. Limits of detection were calculated for an average sample size of 10 grams with 50 ul extracted DNA. Bacteria standard curves had r^2 values of 0.501, 0.368, and 0.107 and the r^2 values for Archaea standards were 0.777 and 0.905. A standard curve from a set of Archaea qPCR analyses is shown below in Figure 2-4.

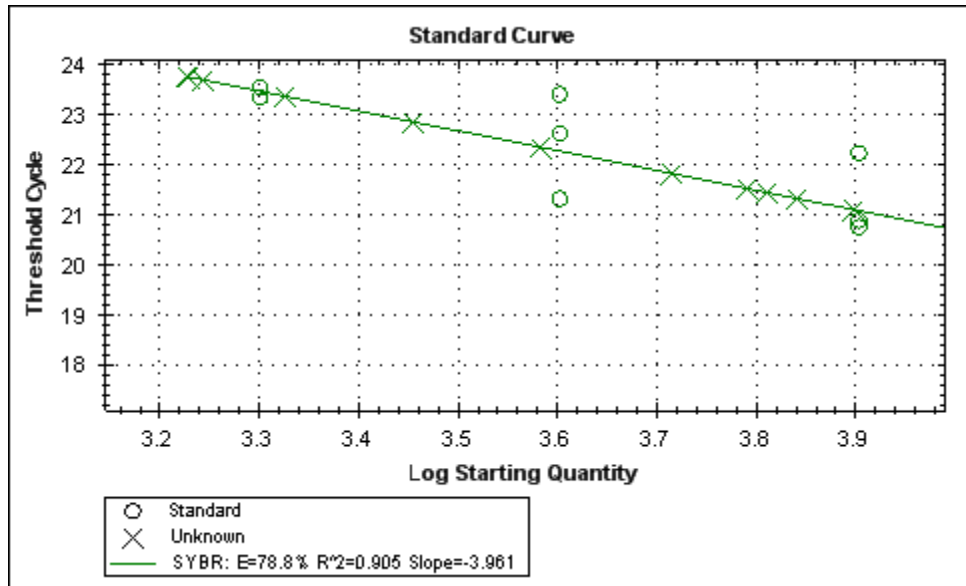


Figure 2-4: Standard curve from Archaea qPCR analyses

Melt curves analyses were performed at the completion of each run to ensure peaks arising from a single PCR product. T-tests were performed to determine the statistical significance of qPCR data.

Terminal Restriction Fragment Length Polymorphism (t-RFLP) Analyses:

To gain an overall sense of community diversity, Terminal Restriction Fragment Length Polymorphism (t-RFLP) was used to assess the diversity of the 16S rRNA gene in a high throughput fashion in both bacteria and Archaea samples. The t-RFLP methodology used in these analyses was previously developed (Brazelton, Schrenk et al. 2006) and optimized towards our specific samples. In these analyses, PCR was performed using a C1000 Thermal Cycler (Bio-Rad) to amplify the terminal fragment of 16S rRNA gene with a fluorescently labeled forward primer. A table of primers (Invitrogen) used for both Archaea and Bacteria t-RFLP are pictured below in Table 2-4.

Table 2-4: Primers Used in t-RFLP analysis (Weisburg, Barnes et al. 1991; Delong 1992)

Primers	Gene Target	Primer Sequence (5'-3')	Size (BP)	Cycling Conditions
B27F	Bacteria 16s rRNA	AGAGTTTGATCCTGGCTCAG	1500	94°C 2 min; 40 cycles: 94°C 30 sec, 54°C
1492R		GGTTACCTTGTTACGACTT		45 sec, 72°C 2 min; 72°C 10 min
1046R - FAM	Bacteria 16s rRNA (V6)	Fam -CGACAGCCATGCANCACT	~1000	94°C 2 min; 33 cycles: 94°C 30 sec, 54°C
Bact518F		CCAGCAGCTGCGGTAAN		45 sec, 72°C 10 min.
B27F-FAM	Bacteria 16s rRNA	Fam - AGAGTTTGATCCTGGCTCAG	1500	94°C 2 min; 33 cycles: 94°C 30 sec, 54°C
1492R		GGTTACCTTGTTACGACTT		45 sec, 72°C 10 min.
Arc21F-FAM	Archaea 16s rRNA	Fam-TTCCGGTTGATCCYGCCGGA	1600	94°C 5 min; 40 cycles: 94°C 30 sec, 55°C
958R		YCCGGCGTTGAMTCCAATT		45 sec, 72°C 2 min; 72°C 6 min.

Each 20 µl PCR reaction contained: 1 µl of template, 1× buffer, 0.2 mM dNTPs, 0.25 µM forward and reverse primers respective to analysis, 1 U *Taq* polymerase, and molecular-grade water to make up the total volume of reaction. Before performing analyses, all samples were screened for Archaea and Bacteria with positively amplifying samples used for downstream analyses. For bacterial t-RFLP, PCR amplification was initially performed using the B27f-1492r primer set. Nested PCR was then performed with the 5-fam 1046R-Bact518f primer set for fluorescent labeling. Archaeal 16S t-RFLP used the 6fam-Arc21f-958r primer set for fluorescent labeling. Once amplified and labeled, the PCR products were purified and digested overnight with restriction enzymes. The restriction enzymes (New England Biolabs Inc.) used in this study are shown below in Table 2-5.

Table 2-5: Restriction Enzymes used in t-RFLP analysis

Enzyme	Cut Site	Temp. (°C)
HAE III	5'GG↓CC	37
	3'CC↑GG	
RSA I	5'GT↓AC	37
	3'CA↑TG	
MSP I	C↓CGG	37
	GGC↑C	
BSTU I	CG↓CG	60
	GC↑GC	

Different sized fluorescently labeled fragments were sequenced and analyzed using GeneMapper system accompanying software (Applied Biosystems).

Peaks analyzed on GeneMapper were then exported and normalized using t-RFLP Analysis Expedited (T-REX) software (Culman, Bukowski et al. 2009). Peaks analyzed were between 50-600 BP in length, and were normalized according to peak height with T-REX software. Community resemblance and similarity analyses were then performed using the Primer6 (PML) software. Two different approaches were used to quantify the compositional dissimilarity between sample sites: Bray Curtis and Jaccard analyses. Resemblance matrices were generated as outputs and were visualized through cluster diagrams.

RESULTS

DNA Quantification

Before beginning molecular analyses DNA was extracted from sulfide samples and quantified to gain an overall account of biomass. Results from DNA quantification are listed below in Table 2-6 which includes predominate samples analyzed in this study.

Table 2-6: DNA Concentration Data

Sample	Chimney	Field	Zone	ng DNA/g sample
1- Eg09 1	El Guapo	Int'l District	Ext	117.62
3- T7-27	S & M	MEF	Ext	54.64
5- t727	S & M	MEF	Ext	92.00
A: F-AT	Finn	Mothra	Ext	349.90
G: Hulk Piece 1	Hulk	MEF	Ext	27.00
G3FeSi	Finn	Mothra	Ext	660.84
FeSi	Finn	Mothra	Ext	1148.48
FeSi 6/25/01	Finn	Mothra	Ext	866.94
FeSi 8/20	Finn	Mothra	Ext	10.53
FG1Fe1	Finn	Mothra	Ext	90.99
FG3Fe	Finn	Mothra	Ext	2.02
3C2 (Inc)	Roane	Mothra	Out	3500.00
8: ALV4017	Hulk	MEF	Mid	72.12
B:FZ2B	Finn	Mothra	Mid	414.23
RnEd 11/18	Roane	Mothra	Mid	909.50
FinnEd	Finn	Mothra	Mid	246.70
Fpyr	Finn	Mothra	Mid	429.42
Fpyr 4/23/01	Finn	Mothra	Mid	264.60
RN2A5 (Inc)	Roane	Mothra	Mid	4435.48
6-F-Z494	Finn	Mothra	Int	150.00
15 - G2pyr-cpy	Finn	Mothra	Int	132.01
C: MEF R-003	n/a	MEF	Bkgd	578.95
D: MEF R-002 (away)	n/a	MEF	Bkgd	210.58
E: MEF R-002 (adj)	n/a	MEF	Bkgd	210.58
9: AIV4021	Hulk	MEF	Bkgd	1.75

Upon examination of DNA concentration values, it was shown that higher DNA concentrations are found within the exterior and middle regions of chimney walls when compared to interior regions ($p = 0.05$).

16S rRNA Taxonomic Screens

PCR assays were performed to identify the presence of 16S rRNA taxonomic genes specific to archaeal and bacterial species. The results of these assays are shown below in Table 2-7.

Table 2-7: Results from 16S rRNA assays for Bacteria and Archaea

Samples	Chimney	Zone	Bac 16s	Arch 16s
1- Eg09 1	El Guapo	Ext	x	
3- T7-27	S & M	Ext	x	x
5: T7-27	S&M	Ext	x	
A: F-AT	Finn	Ext	x	x
G3FeSi	Finn	Ext	x	x
FeSi	Finn	Ext	x	x
FeSi 6/25/01	Finn	Ext	x	x
FeSi 8/20	Finn	Ext		x
FG1Fe1	Finn	Ext	x	x
FG3Fe	Finn	Ext	x	
3C2 (Inc)	Roane	Out	x	x
8: ALV4017	Hulk	Mid	x	
B:FZ2B	Finn	Mid	x	x
RnEd 11/18	Roane	Mid	x	x
FinnEd 11/18	Finn	Mid	x	x
Fpyr	Finn	Mid	x	x
RN2A5 (Inc)	Roane	Mid	x	x
2B6 (Inc)	Roane	Mid	x	x
Fpyr 4/23/01	Finn	Mid	x	x
6-F-2494	Finn	Int	x	
9: AIV4021	Hulk	Bkgd	x	
D: MEF R-002 (away)	n/a	Bkgd		x
E: MEF R-002 (adj)	n/a	Bkgd	x	x

Taxonomic gene assays revealed the presence of both Archaea and Bacteria throughout the hydrothermal chimney gradients.

Archaea and Bacteria qPCR Screens

Bacteria and Archaea qPCR analyses were performed to determine taxonomic 16S rRNA gene abundances throughout chimney gradients. A summary of the results from the bacterial qPCR analysis are shown below in Table 2-8.

Table 2-8: Bacterial qPCR data

Sample	Chimney	Field	Zone	g extract	μl extract	16S copies/ g of sample
3: T7-27	S & M	MEF	Ext	3.02	150	2.48E+04 ± 1.77E4
1- Eg09 1	El Guapo	Int'l District	Ext	2.27	100	1.22E5 ± 1.56E5
G3FeSi	Finn	Mothra	Ext	10.29	50	7.92E+07 ± 6.23E7
FG1Fe1	Finn	Mothra	Ext	10.88	50	8.39E+06 ± 1.76E6
RN2A5	Roane	Mothra	mid	0.62	50	5.53E+07 ± 4.50E7
B: FZ2B	Finn	Mothra	mid	5.13	250	2.95E07 ± 2.29E7
6:F-Z494	Finn	Mothra	Int	5	250	1.66E+06 ± 2.87E6
9: AIV4021	Hulk	MEF	bkgd	3.17	50	7.45E+05 ± 4.93E5

This chart displays gene copies per gram of extracted sample and the extraction data used to generate the final quantity. Samples used in this analysis are mainly from the sulfide chimney Finn, but other deep-sea sulfide samples are included from Roane, Smoke and Mirrors (S&M), El Guapo, and Hulk. Results indicate that there is an even distribution of bacteria 16S rRNA genes throughout middle and exterior chimney gradients.

The summary of results from archaeal qPCR analyses are shown below in Table 2-9.

Table 2-9: Archaeal qPCR data

Sample	Chimney	Field	Zone	g extract	ul extract	16S copies/ g of sample
G3FeSi	Finn	Mothra	Ext	10.29	50	1.07E+08 ± 3.31E7
FeSi	Finn	Mothra	Ext	12.19	50	7.28E+07 ± 4.88E7
A: F-AT	Finn	Mothra	Ext	5.03	250	1.31E+10 ± 8.93E9
FG1Fe1	Finn	Mothra	Ext	10.88	50	9.42E+09 ± 6.18E9
FeSi 8/20	Finn	Mothra	Ext	17.86	50	4.90E+08 ± 1.43E8
FinnEd	Finn	Mothra	Mid	10.6	50	2.95E+08 ± 3.35E7
B: FZ2B	Finn	Mothra	Mid	5.13	250	2.88E+10 ± 1.16E10
Fpyr	Finn	Mothra	Mid	10.98	50	8.34E+09 ± 3.95E9
Fpyr4-23-02	Finn	Mothra	Mid	16.1	50	4.43E+09 ± 2.97E9
RN2A5 (Inc)	Roane	Mothra	Mid	0.62	50	3.01E+10 ± 3.33E8
RnEd	Roane	Mothra	Mid	11.16	50	3.42E+08 ± 2.65E7

As seen in the bacteria qPCR data, the majority of samples used in these analyses were from the sulfide chimney Finn, with two samples originating from the chimney Roane found within the same vent field, Mothra, as Finn. Looking at the relative gene abundances of the throughout different chimney gradients there also appears to be an even distribution of Archaea 16S rRNA genes.

A summary chart comparing Archaea and Bacteria 16S rRNA gene abundance data from this study is shown below in Figure 2-5.

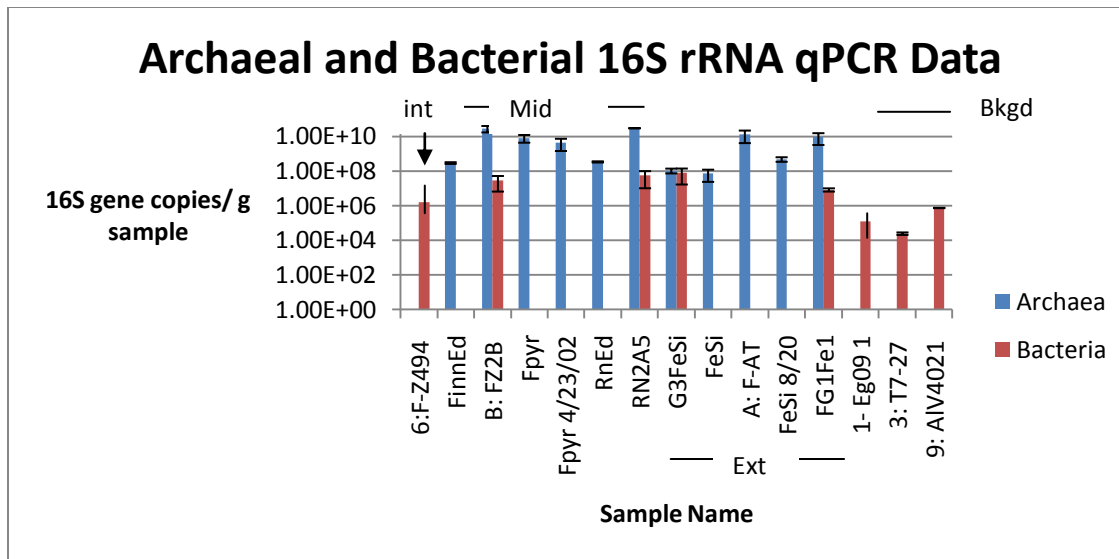


Figure 2-5: Archaea and Bacteria qPCR summary chart

Overall there was a higher abundance of archaeal 16S rRNA genes than bacterial 16S rRNA genes assayed ($p = 0.017$). Four pairs of samples were assayed in both bacteria and Archaea 16S rRNA qPCR analyses. Ratios of Archaea 16S rRNA genes to bacterial 16S rRNA genes were generated to gain an idea of overall species abundance. The table of ratios is shown below in Table 2-10.

Table 2-10: Archaea:Bacteria gene abundance ratios throughout chimney samples

Sample	Chimney	Zone	Arch:Bac Ratio
B: FZ2B	Finn	Mid	977.92
RN2A5 (1:10)	Roane	Mid	544.33
G3FeSi	Finn	Ext	1.35
FG1Fe1	Finn	Ext	1122.72

Within these specific samples Archaea genes outnumber bacterial genes from 1-to-1000 times. Using a complete data set of bacterial samples below detection limit in this study showed significantly higher levels of Archaea than bacterial 16S rRNA genes within middle chimney

gradients ($p = 0.05$). These data cement the fact that there are higher amounts of Archaea throughout the hydrothermal chimney samples assayed in this study.

T-RFLP Analyses

t-RFLP analyses were conducted for both Bacteria and Archaea to gain a sense overall microbial diversity throughout chimney gradients and other hydrothermal systems. As mentioned previously in t-RFLP methods, two community approaches were used, Bray Curtis and Jaccard Analyses. Both methods yielded similar results therefore only Bray-Curtis outputs are displayed. A summary of samples used in bacteria t-RFLP analyses is shown below in Table 2-11.

Table 2-11: Sample summary for bacteria t-RFLP analyses

Chimney	Zonation	Sample	Enzyme	Total Peaks
Finn	Exterior	A F-AT	BSTU I	18
Finn	Exterior	A: F-AT	HAE III	18
Finn	Exterior	FeSi	HAE III	31
Finn	Middle	B: FZ2B	BSTU I	27
Finn	Middle	B: FZ2B	HAE III	34
Finn	Middle	Finn Ed 11/18	BSTU I	21
Finn	Middle	Finn Ed 11/18	HAE III	23
Hulk	n/a	8: ALV4017	BSTU I	28
Hulk	n/a	8: ALV4017	HAE III	26

Most of these samples are from the sulfide Finn, but a few samples are representative of the chimney Hulk. Both chimneys are from different vent fields located off the JdFR. Samples from Finn were collected throughout different gradients while Hulk samples contained homogenized sulfide, not restricted to any particular gradient. Through bacterial t-RFLP analysis, two restriction enzymes were successful in generating fragments for downstream community analyses, *Hae* III and *Bstu* I. For each enzyme both the Bray-Curtis and Jaccard community analyses were used generating community similarity matrices to ensure a consistency in analysis

methods. For each sample, the total number of fragment peaks generated through t-RFLP analysis gives an idea of its overall species richness/ organism diversity; these are shown in Table 2-11 above. The *Hae III* digestion of FZ2B generated the most peaks and therefore had the highest species richness. Samples from Hulk also showed a high number of peaks as well demonstrating that samples from different chimney environments can have similar levels of species richness. All of the other samples were pretty rich in comparison. The similarity matrix generated through the Bray-Curtis *Hae III* fragment analysis is shown below in Table 2-12.

Table 2-12: Matrix generated through Bray-Curtis community similarity analysis for the *Hae III* digestion of Bacteria t-RFLP products

	10_HAE_B02.fsa	12_HAE_D02.fsa	13_HAE_E02.fsa	8_HAE_H01.fsa	9_HAE_A02.fsa
10_HAE_B02.fsa: ALV4017	100.00	16.39	8.23	70.39	10.65
12_HAE_D02.fsa: Finn Ed	16.39	100.00	8.86	20.08	10.98
13_HAE_E02.fsa: FeSi	8.23	8.86	100.00	19.87	82.35
8_HAE_H01.fsa: F-AT	70.39	20.08	19.87	100.00	21.53
9_HAE_A02.fsa: FZ2B	10.65	10.98	82.35	21.53	100.00

A visual representation of the matrix is represented in the cluster diagram pictured below in Figure 2-6.

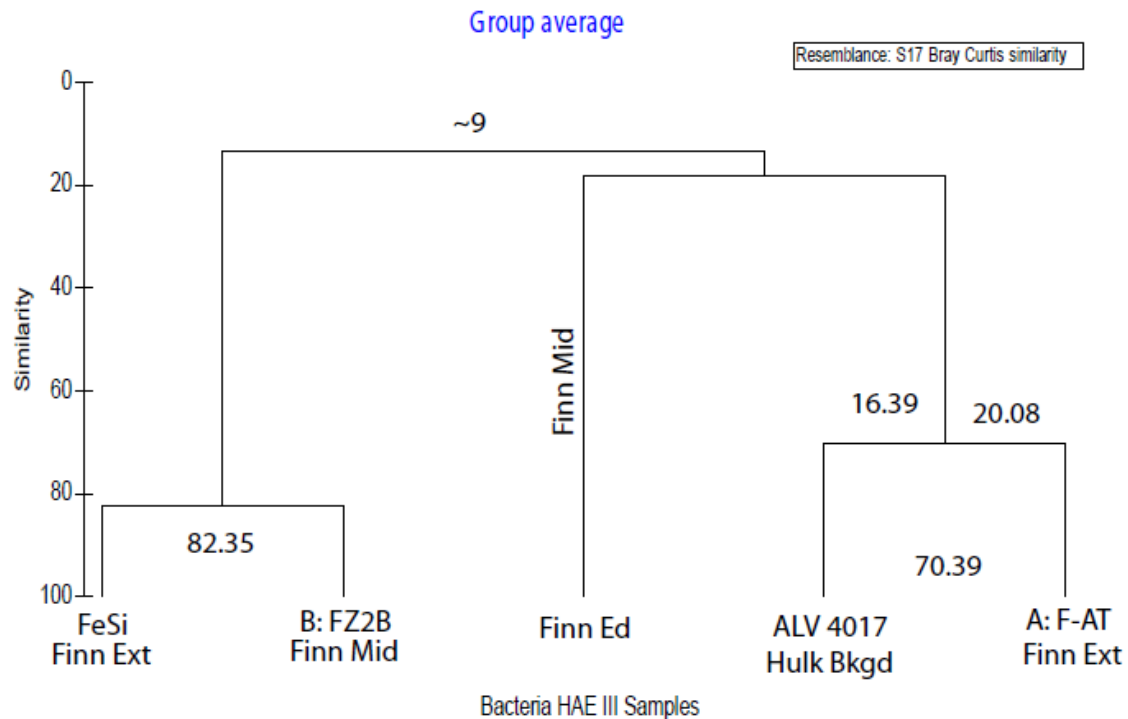


Figure 2-6: Cluster diagram generated through Bray-Curtis community similarity analysis for the *Hae* III digestion of Bacteria t-RFLP products

It is shown that through this sample distribution there is a high level of heterogeneity within bacteria communities. Samples are clustered together from different chimneys, ALV4017 and F-AT, while communities from the same chimney are clustered apart. The sample Finn Ed from Finn's middle gradient serves as an outlier community with little to no overlap with others. This leads to the suggestion that there may be an environmental influence upon bacteria community dispersion.

The next set of analyses also pertained to bacteria t-RFLP, but these analysis used looked at fragments generated through *Bstu* I digestion. The FeSi from Finn's exterior was not included

in this analysis because it lacked a *Bst* I digest fragment. The Bray-Curtis community analysis matrix for the *Bst* I digestion of bacteria t-RFLP products is shown below in Table 2-13.

Table 2-13: Matrix generated through Bray-Curtis community similarity analysis for the *Bst* I digestion of Bacteria t-RFLP products

	10_BSTU_A07.fsa	12_BSTU_C07.fsa	8_BSTU_G06.fsa	9_BSTU_H06.fsa
10_BSTU_A07.fsa: ALV4017	100.00	0.24	92.05	82.67
12_BSTU_C07.fsa: Finn Ed	0.24	100.00	0.00	4.52
8_BSTU_G06.fsa: F-AT	92.05	0.00	100.00	81.31
9_BSTU_H06.fsa: FZ2B	82.67	4.52	81.31	100.00

The corresponding cluster diagram is shown below in Figure 2-7.

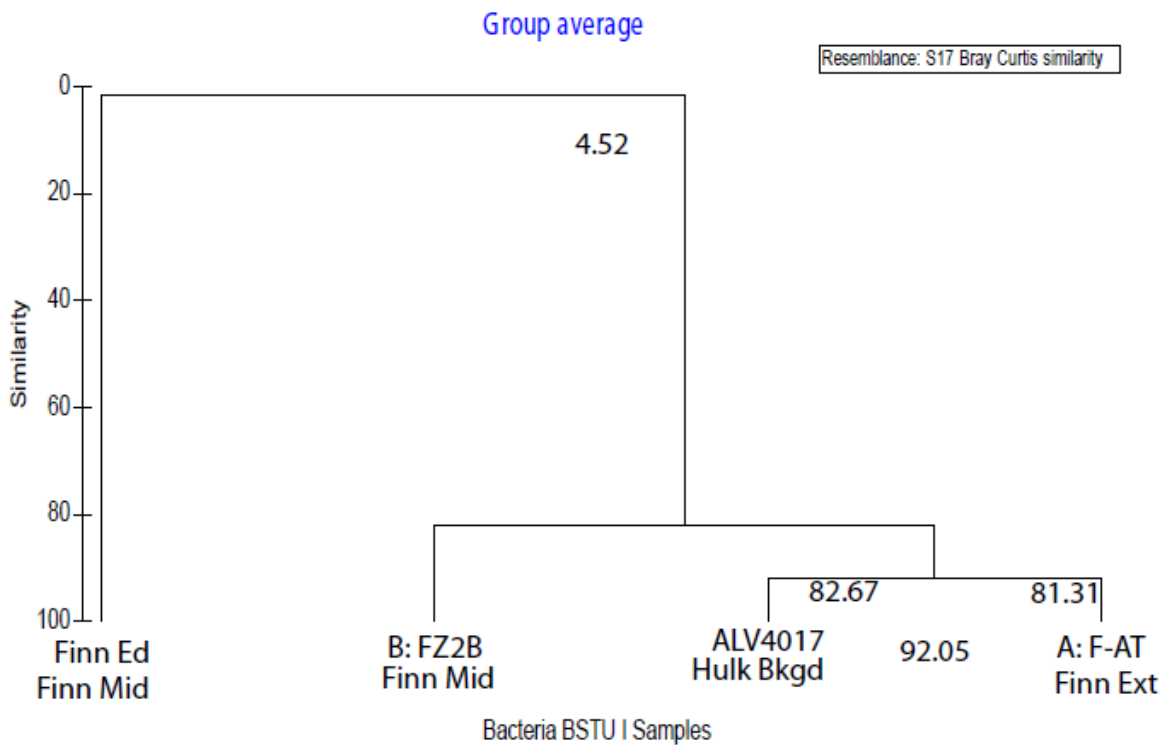


Figure 2-7: Cluster diagram generated through Bray-Curtis community similarity analysis for the *Bst* I digestion of Bacteria t-RFLP products

This diagram once again shows the clustering of ALV 4017 and F-AT from different chimneys and the Finn Ed outlier community. One major difference is that now FZ2B, grouped apart in the previous *Hae* III digestion is now grouped with the ALV4017 and F-AT cluster. Dissimilarities in the two different t-RFLP digests could be attributed to issues stemming from incomplete digestion on either end. Looking at both t-RFLP community analyses there is still a high level of heterogeneity potentially stemming from environmental influence.

Archaeal 16s t-RFLP analysis was conducted similarly for bacteria except using primers specific for the archaeal 16s rRNA gene. Archaea samples analyzed in this study are displayed below in Table 2-14.

Table 2-14: Sample summary for Archaea t-RFLP analysis

Chimney	Zonation	Sample	Temp	Total Peaks
Finn	Exterior	G3FeSi	302	14
Finn	Exterior	FeSi	302	37
Roane	middle	RnEd	200	25
Finn	middle	Finn Ed	302	31

All samples except for sample RnEd from Roane were from the sulfide chimney Finn. Roane and Finn are both chimneys from the same hydrothermal vent field, Mothra, off the JdFR. Upon examination of total peaks, samples FeSi, and Finn Ed had the most species richness in the both exterior and middle gradients of Finn respectively. The Roane sample was not as rich therefore having potentially less species diversity within than Finn. G3FeSi, showed very low diversity when compared to the other samples. Only one restriction enzyme, *Rsa* I, successfully digested usable fragments from Archaea t-RFLP products digestion. The Bray-Curtis community similarity matrix generated through the analysis of *Rsa* I Archaea t-RFLP is shown below in Table 2-15.

Table 2-15: Matrix generated through Bray-Curtis community similarity analysis for the *Rsa* I digestion of t-RFLP products

	2_RSA_D04.fsa	4_RSA_F04.fsa	5_RSA_G04.fsa	6_RSA_H04.fsa
2_RSA_D04.fsa: G3FeSi	100.00	8.79	10.82	58.36
4_RSA_F04.fsa: RnEd	8.79	100.00	49.68	7.63
5_RSA_G04.fsa: Finn Ed	10.82	49.68	100.00	17.29
6_RSA_H04.fsa: FeSi	58.36	7.63	17.29	100.00

The corresponding cluster diagram is shown below in Figure 2-8.

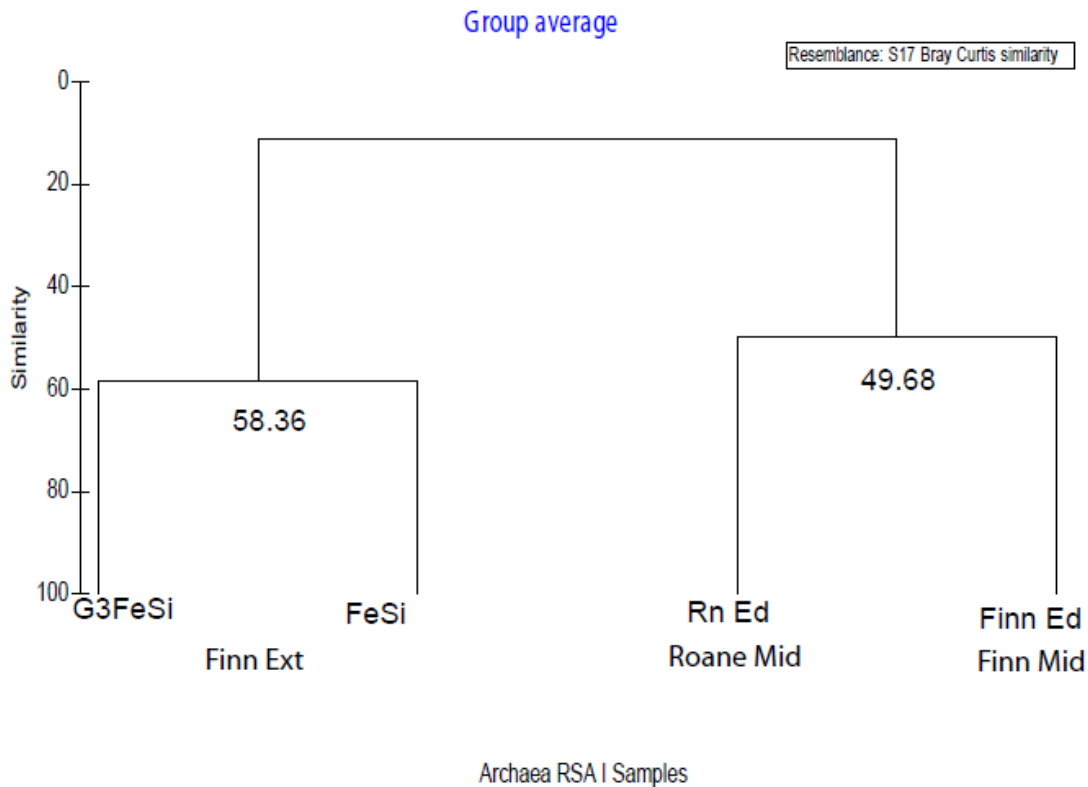


Figure 2-8: Cluster diagram generated through Bray-Curtis community similarity analysis for the *Rsa* I digestion of Archaea t-RFLP products

Cluster diagrams indicate that the Archaea communities of samples RnEd and Finn Ed and of samples G3FeSi and FeSi have overlap amongst themselves, but these sets are dissimilar from one another. Communities grouped together are from the same chimney gradients. Even though source chimneys may differ, it can be seen that specific gradients harbor different communities of Archaea therefore suggesting a possible environmental gradient influence on archaeal community dispersal.

DISCUSSION

Microbial community analyses were used to determine overall microbial community structure throughout hydrothermal vents. Samples analyzed came from a vast array of chimneys and gradients in order to provide a systematic approach to assess and compare the distinct environments within these systems. These analyses were conducted using many different types of methodology to gain a thorough picture of the overall environmental community structure. Through these analyses, a number of conclusions can be drawn.

Initial analyses aimed towards extracting and quantifying DNA from a multitude of hydrothermal chimney samples. Overall results indicate higher biomass quantities found within exterior and middle chimney gradients. This is likely due to the fact that these lower temperature regions allow for the growth of mesophilic to thermophilic organisms as opposed to the high temperature, uninhabitable regions towards chimney interior zones, next to active venting processes. This was expected from these samples because previous studies have shown higher cell abundance data towards middle and exterior portions of chimney walls when compared to interior portions (Schrenk, Kelley et al. 2003).

Further analyses were aimed towards the quantification of taxonomic genes specific to Archaea and Bacteria through qPCR methodology. Through interpretation these data, it was shown that there was a consistent distribution of both Archaea and Bacteria throughout middle and exterior chimney gradients. Comparing Archaea gene abundance data to Bacteria gene data it was shown that there were elevated archaeal gene abundances amongst samples analyzed especially within middle chimney gradients. This could be attributed to specific environmental adaptations of Archaea making better equipped to cope and thrive amongst hydrothermal conditions. Previous studies have shown that thermophilic to hyperthermophilic Archaea species

are more prevalent towards interior regions hydrothermal chimney structure (Takai, Komatsu et al. 2001; Schrenk, Kelley et al. 2003). Due to their intense thermal habitats, it has been hard to culture Archaea; therefore, genetic analyses help gain insight into overall Archaea distribution and abundance. This study only scratches the surface of Archaea abundance in chimney environments. In order to gain a better handle on Archaea gene abundance data throughout hydrothermal chimney walls, downstream analyses need to utilize a larger data set encompassing the full span of chimney gradients amongst multiple vent systems.

To gain a further understanding of community distributions specific to Archaea and Bacteria analyses were conducted to gain a sense of community similarity and overall diversity amongst chimneys and the gradients throughout. This was determined through the use of t-RFLP analyses on archaeal and bacterial taxonomic genes. It was inferred through these analyses that there are specific factors that play a role in the growth of specific types in microbial communities. These factors can depend of the particular gradient itself or specific chemical and physical conditions of the ecological niche placing a first order control on the types of microbial communities that exist (Schrenk, Kelley et al. 2003). Both bacterial and archaeal community dispersal patterns experience high heterogeneity. In order to constrain which factors affect microbial community dispersal, larger sample sets and the use of more restriction enzymes will provide a more complete picture. Looking at the overall species richness of samples in general, richness varied throughout different chimneys and samples. Samples with the highest species richness were found in middle to interior chimney zones. This is due to the fact that middle regions of the chimney wall are believed to experience high diversity due to their location directly between the cold SW and hot HF barriers. Middle chimney gradients experience the

highest level of fluid mixing and disequilibrium, generating large amounts of free energy allowing for the growth of a diverse array of organisms (McCollom and Shock 1997).

In summary, hydrothermal environments harbor substantial diversity with both archaeal and bacterial species. Dispersal of microbial communities has not been constrained. In order to gain a sense of overall community dispersal, a longitudinal study of multiple vents and specific gradients needs to be investigated. The localization of these species can be due to a multitude of environmental controls, dependent on physical and chemical conditions of the specific chimney gradient. Through the elucidation of these factors, more clues can be used to establish the dispersal and overall uniqueness of microbial communities throughout hydrothermal chimney walls.

CHAPTER III: TAXONOMIC COMPARISON OF HYDROTHERMAL CHIMNEY MICROBIAL COMMUNITIES

INTRODUCTION

Hydrothermal chimneys are diverse habitats both on local and global scales. These habitats can sustain organisms from thermophiles to psychrophiles and from strict anaerobes to aerobes (Schrenk, Holden et al. 2008). Despite dozens of studies of the microbiology of deep-sea hydrothermal chimneys, a consistent picture of microbial community patterns or the factors dictating their compositions has not yet emerged. Studies on chimney ecosystems have been conducted throughout multiple deep-sea vent fields throughout the world including culture-dependent and independent means of determining microbial diversity through phylogenetic analyses, biomass measurements, and obtaining biosignatures (Schrenk, Holden et al. 2008). In addition to diversity studies, geochemical studies have been performed on chimneys and hydrothermal fluid dynamics (Schrenk, Holden et al. 2008). Amongst these studies an overall synthesis of information has yet to emerge. This study aims towards the establishment of a link determining which factors, either environmental or geographical, influence the distribution and diversity of vent chimney inhabitants. This investigation compiles existing data from databases of 16S rRNA sequences to compare similarities between vent ecosystems both locally and globally. Subsequently, the occurrence of putative autotrophic taxa was evaluated in terms of the community compositions.

A general trend reported from individual studies of vent chimneys, including those reported in Chapter II of this thesis, is a decrease in cell concentrations, proceeding from the exterior to the interior of a hydrothermal chimney wall. The community composition has also been shown to generally shift from bacterial dominated in exterior regions, to archaeal

dominated in interior regions (Schrenk, Holden et al. 2008). The greatest microbial community diversity has been shown in middle regions of mature chimney structures (Schrenk, Holden et al. 2008), which likely contain a multitude of energy sources, and organic carbon from both in situ production and buried macrofaunal biomass. Commonly reported taxa from vent chimney environments include *Epsilonproteobacteria*, which can range from mesophiles to thermophiles (Nakagawa and Takai 2008). *Epsilonproteobacteria* are common hydrogen and sulfur oxidizing organisms, and can accumulate to high densities in the shallow hydrothermal vent subsurface as well (Campbell, Engel et al. 2006). *Gammaproteobacteria* are also frequently reported in the vent chimney habitat, and commonly occur as symbionts with vent macrofauna, such as tube worms. Archaeal species found in the vent habitat include hyperthermophilic Crenarchaeota which catalyze hydrogen and sulfur oxidation near the upper temperature limits to life (~122°C), and heterotrophic, thermophilic Euryarchaeota such as Thermococcales (Madigan and Martinko 2006). There are also numerous reports of “uncultured Archaea,” whose identity is only known through their 16S rRNA gene sequence, with no associated physiological or metabolic data (Schrenk, Holden et al. 2008).

The polymerase chain reaction (PCR), cloning, and sequencing of prokaryotic ribosomal RNA genes (16S rRNA) has become a mainstay of environmental microbiology over the last 20 years, offering a convenient and reliable taxonomic marker for microbial communities. Sequences obtained from cloning have accumulated in public databases with various levels of annotation. Qualitatively, there does not appear to be any consistency in the taxonomic composition of chimney hosted microbial communities (Schrenk, Holden et al. 2008), which make it difficult to decipher whether environmental conditions select for specific communities, or if there is an overriding geographic component.

The design of sequence analysis software has provided a tool for microbial ecologists to explore patterns in community composition between samples and eventually output information that is comparable with multi-variate analyses. MOTHUR, a software program developed by Dr. Patrick Schloss at the University of Michigan, takes complex sequence data sets and converts them to visuals to allow for the examination of microbial community overlap and the distribution of particular operational taxonomic units (OTU's) or species at different levels (Schloss, Westcott et al. 2009). Through this study, the use of MOTHUR software provided a means to compile and organize a large dataset and turn it into a manageable form for community comparison.

OBJECTIVES

The overarching objectives of this chapter are to evaluate the overlap between microbial populations in different studies of hydrothermal vent chimneys at various degrees of taxonomic resolution. Specifically, I will:

- 1.) Evaluate whether a core microbial community exists that is common to all deep-sea hydrothermal chimney sites, and
- 2.) To look for patterns between community composition and habitat characteristics of the various hydrothermal vent chimney samples.

HYPOTHESES

In order to address these objectives, I will test the following hypotheses in this chapter:

- 1.) Chimney age and geographical location influence hydrothermal chimney microbial composition:
 - a. young organic-poor chimneys form distinct chemolithoautotrophic microbial communities relative to mixotrophic communities of mature (evolved) organic-rich chimneys
 - b. Chimneys from different geographic regions will harbor distinct microbial communities.
- 2.) Archaeal and bacterial communities display similar distributions throughout chimney wall ecosystems.

MATERIALS AND METHODS

Compiling Clone Sequences

Microbial community compositions obtained by 16S rRNA sequencing were compiled from GenBank (NCBI) using the accession numbers found in published studies of deep-sea hydrothermal vents. These sequences were exported from GenBank in FASTA format and aligned using the alignment program in Greengenes (DeSantis, Hugenholtz et al. 2006).

MOTHUR Community Analyses

Compiled sequences were analyzed using MOTHR (Schloss, Westcott et al. 2009) to determine community similarities. This program works to analyze complex data sets and convert them to visuals to compare different microbial ecosystem structures (Schloss, Westcott et al. 2009). Preliminary data from previous work on sulfide chimneys was used to generate a database that served as a comparison between different hydrothermal systems. This provides a reference data set for downstream analyses of hydrothermal ecosystems. The complete data set is comprised of bacterial and archaeal sequences from clone libraries of SSU 16S rRNA gene sequences.

Tree files generated through analyses were visualized in TreeView (Roderic D. M. Page, Taxonomy and Systematics at Glasgow) and modified in Adobe Illustrator. Matrices describing the occurrence of specific sequences across samples were observed and queried in Microsoft Excel to identify overlapping taxa. A summary of microbial diversity studies in which 16S rRNA clone libraries were incorporated for this study are summarized below in Table 3.1.

Table 3-1: Microbial diversity studies of vent chimneys used in the MOTHUR analyses

Location	Site Name	Sample	Temp. °C	Reference
Southern Mariana Trough	Fryer	SMT-F1 to F5	107	Kato et al., 2010
	Archaean	SMT-Acs1 to Acs3	117	Kato et al., 2010
	Pika	SMT-Pbs1 to Pbs4	270	Kato et al., 2010
		SMT-Pcs1 to Pcs 3	19	Kato et al., 2010
		SMT-PltB, G, O	2	Kato et al., 2010
Juan de Fuca Ridge		SMT-YdcB, G	2	Kato et al., 2010
	Axial Volcano	AxVolc-CH	35	Page et al 2004
	Mothra Vent Field	JdFR-FZ1	2-20	Schrenk et al 2003
		JdFR-FZ2	ND	Schrenk et al 2003
		JdFR-FZ3	150-302	Schrenk et al 2003
		Roane- inc.	25 - 250	Schrenk, unpub.
	Main Endeavour Field	Hulk- inc.		Schrenk, unpub.
Mid-Atlantic Ridge	Snake Pit	MAR-SnkP	20-70	Reysenbach et al. 2000
Manus Basin	PACMANUS	PACMA	250	Takai et al 2001
East Pacific Rise	9°N	CH1 - Ch9	350	Kormas et al., 2006
		EPR-PROTO	98-203	McCliment et al. 2006
		EPR-a125	35-144	McCliment et al. 2006
		EPR-FP	40-180	McCliment et al. 2006
		EPR-POT	350	McCliment et al. 2006
		EPR-IVO	223	McCliment et al. 2006
Guaymas Basin	Broken Mushroom and Toadstool Vent	Guay-BMT	110-302	Page et al 2008
		GB	30-100	McCliment et al. 2006

There is great diversity amongst chimney sites sampled encompass diverse venting temperature, chimney classifications scattered throughout different locations throughout the world. A map depicting different sampling locations is shown below in Figure 3-1.

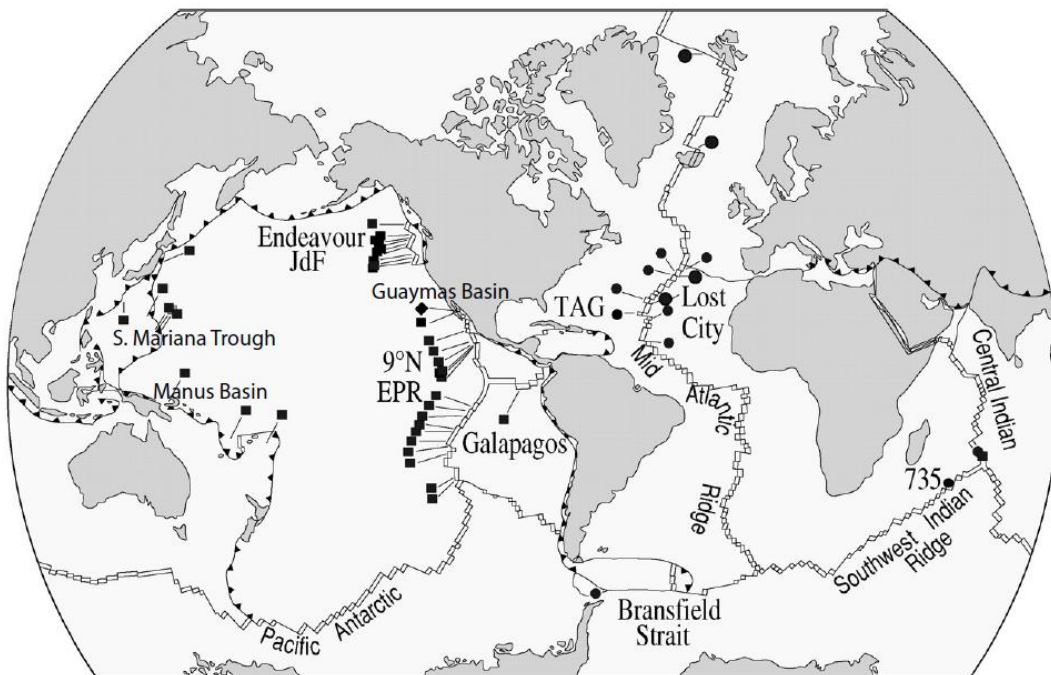


Figure 3-1: Map depicting locations of sampling sites used for the generation of clone libraries utilized in this study (Kelley, Baross et al. 2002).

The specific 16S rRNA sequence data input into MOTHUR software is summarized below in Table 3-2.

Table 3-2: Microbial 16S rRNA sequence data incorporated into the study

Location	Site Name	Arch	Bac	Accession Number (GenBank)	Reference
		# of seqs	# of seqs		
Southern Mariana Trough	Fryer	100	636	AB424684:AB425028; AB292856:AB293246	Kato et al., 2010
Juan de Fuca Ridge	Axial Volcano	15	64	AY280373:AY280451	Page et al 2004
	Mothra Vent Field	228	23	AY165965:AY166119; DQ228532:DQ228554	Schrenk et al 2003
		17	-	DQ228515:DQ228531	Schrenk, unpub.
		48	37	DQ228584:DQ228632; DQ228633:DQ228669	Schrenk, unpub.
	Main Endeavour Field	160	-	nr	Lin, unpub.
Mid-Atlantic Ridge (MAR)	Snake Pit	12	32	AF068782:AF068824, AF209779	Reysenbach et al. 2000
Manus Basin	PACMANUS	22	-	AB052972:AB052993	Takai et al 2001
East Pacific Rise (EPR)	9°N	35	44	AY672497-AY672540; AY672462-AY672496	Kormas et al., 2006
		30	-	DQ122674:DQ122703	McCliment et al. 2006
Guaymas Basin	Broken Mushroom and Toadstool Vent	89	-	DQ925926:DQ926006; DQ925859:DQ925866	Page et al 2008
<i>total</i>		756	836		

Through the compilation of data from GenBank, 756 and 836, archaeal and bacterial sequences respectively were analyzed using MOTHUR.

RESULTS

Bacteria MOTHUR Analysis

Amongst the bacteria, 836 sequences were compiled and analyzed in MOTHUR generating a cluster diagram seen in Figure 3-2. A similarity threshold of 90% was used to define OTU's, which corresponds roughly to the order level in prokaryotic taxonomy.

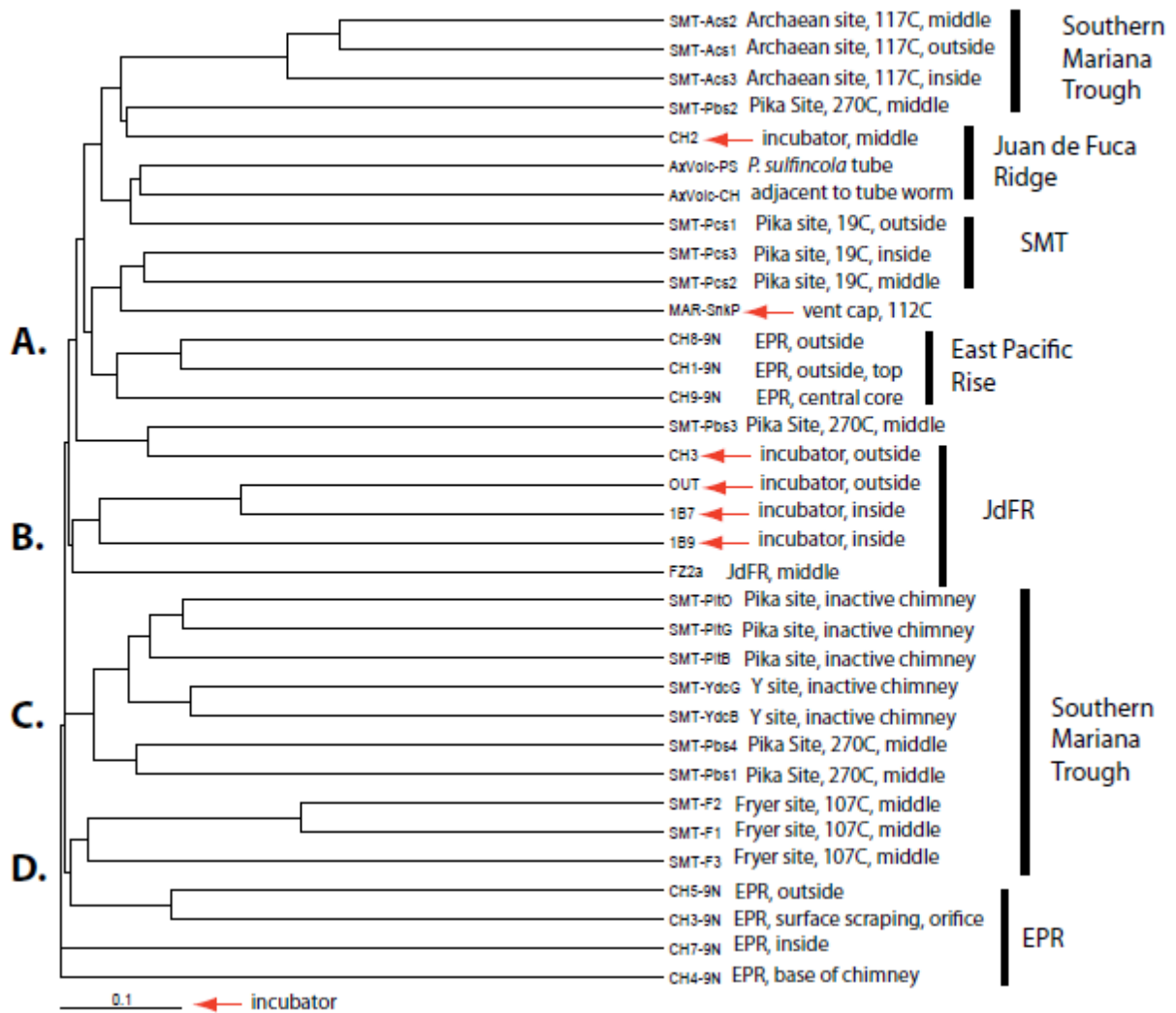


Figure 3-2: Cluster diagram showing the similarity of bacterial communities in different hydrothermal chimneys and in situ incubators using an OTU cutoff of 90%.

Through the investigation of the bacteria cluster diagram, it appears that sequences were grouped together based on their geographic locations. Sequences from the same chimney grouped together as a unit, suggesting that bacteria community distribution may have a geographic basis. The cluster diagram was broken up into four distinct clusters to perform a composite analysis looking at community overlap between main sequence groupings. A summary of community overlap between key clusters are shown below in Table 3-3.

Table 3-3: Distribution of bacterial OTU's in composite analysis

Distribution of Bacterial OTU's in Composite Analysis				
	A	B	C	D
<i># of sequences</i>	507	39	240	50
<i>Aquificales-like</i>	x			x
<i>Thermus-like</i>	x		x	
<i>Alphaproteobacterium</i>	x		x	
<i>Alphaproteobacterium</i>				x
<i>Gammaproteobacterium</i>			x	x
<i>Gammaproteobacterium</i>	x	x	x	
<i>Gammaproteobacterium</i>	x	x	x	
<i>Gammaproteobacterium</i>	x		x	
<i>Deltaproteobacterium</i>	x		x	
<i>Epsilonproteobacterium</i>	x			
<i>Epsilonproteobacterium</i>	x			
<i>Epsilonproteobacterium</i>	x		x	
<i>Epsilonproteobacterium</i>	x	x		
<i>Epsilonproteobacterium</i>	x			x
<i>Epsilonproteobacterium</i>	x		x	
<i>Sulfurimonas-like</i>	x			
<i>Sulfurovum-like</i>	x			x
<i>Bacterioidetes-like</i>	x		x	
<i>Bacterioidetes-like</i>		x		
Operational Taxonomic Units (OTU's) Defined as >90% sequence similarity				

Key clusters include the groupings A, B, C, and D which predominately have a geographic basis. Group A has natural chimneys and a few incubator samples with high vent

fluid temperatures from the Southern Mariana Trough (SMT), and the East Pacific Rise (EPR), with a few chimney samples from cooler tubeworm-dominated regions of the Juan de Fuca Ridge (JdFR). Group B contains incubator samples from the JdFR from both the Finn and Roane chimneys of the Mothra field with a range of vent fluid temperatures from 25-250°C. Group C contains natural chimney samples from the SMT with a vent fluid temperatures range of 2°C-270°C. Group D has samples from both the SMT and the EPR with vent fluid temperatures of 107°C and 350°C.

Main groupings of bacteria OTU's include thermophiles, *Proteobacteria*, and common marine bacteria species. Upon examination of sequence overlap among bacteria OTU's, there are few cluster distribution patterns that can be deduced including bacteria groups confined to one particular cluster and some that are cosmopolitan which can adapt to a variety of clusters.

Amongst thermophiles there are two distinct groupings, *Aquificales* and *Thermus*-like bacteria found in clusters A, C, D. Both of these groups are found with the higher temperature A cluster with some overlap into the C and D clusters which also contain high temperature sites.

Among *Proteobacteria* OTUs, *Gammaproteobacteria* and *Epsilonproteobacteria* OTUs were found in high abundance throughout vent studies. *Proteobacteria* are a very diverse phylum containing a multitude of different species types with vast metabolic diversity physiological adaptations depending on species type (Madigan and Martinko 2006). *Gammaproteobacteria* in this comparative study were pretty cosmopolitan in nature but were overlapping predominately in the natural chimney clusters A and C while *Epsilonproteobacteria* were scattered throughout a few chimney systems, but were mainly confined to the thermophilic cluster A.

Marine bacteria included in the study were *Epsilonproteobacteria* subgroups *Sulfurimonas* and *Sulfurovum*-like OTUs, and *Bacteroidetes*-like OTU's. Upon examination of

the *Sulfurimonas* and *Sulfurovum*-like OTU'S, these appear to be confined to the higher temperature A cluster while *Bacterioidetes*-like groups were overlapped throughout clusters B and C indicative of incubators, and low vent temperature environments.

Archaea MOTHUR Analysis

Among Archaea, 756 total sequences were assembled from the studies described in Table 3.1 were downloaded from GenBank and analyzed using MOTHUR. The results are summarized visually through a cluster diagram represented in Figure 3-3. A similarity threshold of 90% was used to define OTU's.

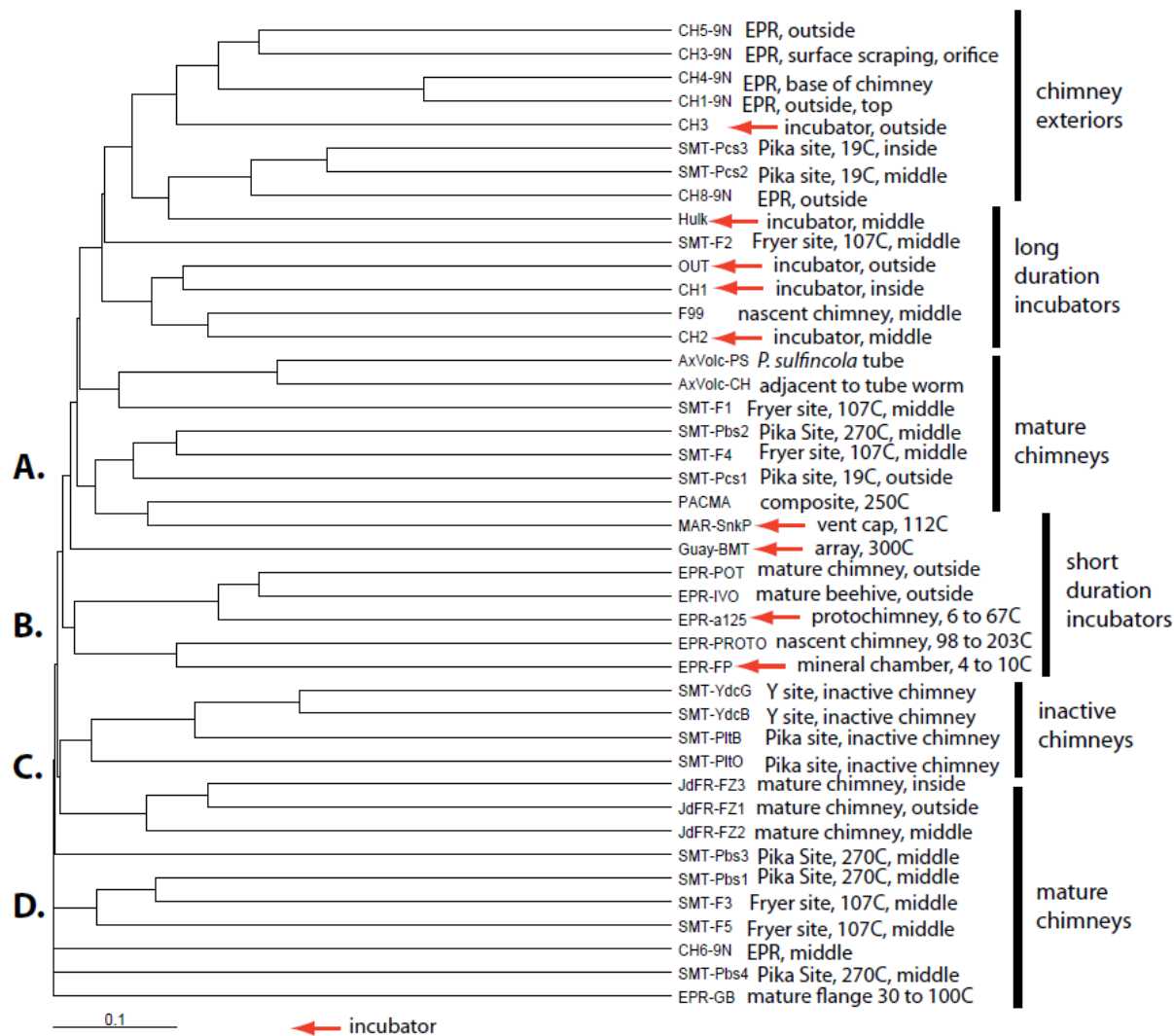


Figure 3-3: Cluster diagram showing the similarity of archaeal communities in different hydrothermal chimneys and in situ incubators using an OTU cutoff of 90%.

Through the investigation of the Archaea cluster diagram, it appears that distinct groupings of sequences were grouped together based on environmental conditions from their indigenous chimney environment. Therefore environmental influence may play a role on archaeal community distribution. It is shown throughout the diagram that there are distinct clusters representative of specific stages of chimney development and “lifespan.” These include

the A cluster which include exterior chimney gradients, long duration incubators, and mature “white smoker” chimney environments. Cluster B contains short-duration incubator, and nascent chimney sequences. Cluster C contains sequences from inactive chimneys and cluster D contains OTU’s from mature chimneys. The cluster diagram was broken up into these four clusters to perform a composite analysis to look at community overlap between clusters. A summary of community overlap between key clusters are shown below in Table 3-4.

Table 3.4: Distribution of archaeal OTU's in composite analysis

Distribution of Archaeal OTU's in Composite Analysis				
Group	A	B	C	D
# of Sequences	376	119	247	14
Korarchaeote-like	x		x	
Marine Group I Crenarchaeote			x	
Marine Group I Crenarchaeote	x			x
uncultured marine Crenarchaeote		x	x	
uncultured marine Crenarchaeote			x	
uncultured benthic Crenarchaeon	x		x	
uncultured vent Crenarchaeote	x			x
uncultured vent Crenarchaeote			x	
uncultured vent Crenarchaeote (x2)	x		x	
<i>Desulfurococcus</i> -like	x			
<i>Vulcanisaeta</i> -like	x			
<i>Thermofilum</i> -like	x		x	
<i>Staphylothermus</i> -like	x			
<i>Thermoproteus</i> -like	x			x
<i>Ignicoccus</i> -like	x	x		
uncultured Euryarchaeote				x
Marine Group II Euryarchaeote	x			
<i>Haloarcula</i> -like	x			
uncultured vent Euryarchaeon (x4)			x	
uncultured vent Euryarchaeote		x	x	
uncultured vent Euryarchaeote	x	x		
uncultured vent Euryarchaeote	x		x	
uncultured chimney Euryarchaeote			x	
<i>Archaeoglobus fulgidus</i> -like	x			x
<i>Archaeoglobus</i> -like	x		x	
<i>Archaeoglobus</i> -like	x	x		
<i>Methanocaldococcus</i> -like		x		
<i>Methanocaldococcus</i> -like		x		
<i>Aciduliprofundum</i> -like	x			
<i>Thermococcus</i> -like	x	x	x	
<i>Thermococcus</i> -like (x2)	x			
<i>Nanoarchaeote</i> -like (x2)		x		
Operational Taxonomic Unit (OTU) defined as >90% sequence identity				

Predominant Archaea OTU's include Marine Group I Crenarchaeota, uncultured Crenarchaeota, *Archaeoglobus*, and *Thermococcus*. As mentioned previously, Archaea in the form of Crenarchaeota have two distinct groups in chimney ecosystems including Marine Group I (MGI) benthic organisms found towards exterior chimney regions and hyperthermophiles found towards interior chimney regions (Schrenk, Holden et al. 2008). In this compilation two different groups were found, cultured MGI and uncultured Crenarchaeota. The cultured Crenarchaeota OTU's differed in that they grouped among different clusters. One type of OTU grouped among the C cluster - inactive chimneys, while one particular OTU grouped with A and D - mature chimneys. This can demonstrate MGI's confinement to lower temperature, benthic-like chimney regions. On the other hand the uncultured Crenarchaeota were very cosmopolitan due to their overlap in all clusters particularly in inactive chimneys. This could be attributed to their versatile physiology (Madigan and Martinko 2006).

The hyperthermophilic *Archaeoglobus* and *Thermococcus* OTU groupings are found predominately within mature cluster A. Some OTU's are restricted to specific clusters while other span throughout all clusters. These demonstrate a level of versatility and a level of confinement which may be influenced by environmental factors.

DISCUSSION

Controls upon Microbial Community Composition in the Vent Chimney Habitat

Both geographic and environmental factors appear to impact the composition of microbial communities in the vent chimney environment. Amongst the Bacteria, the geographic distribution of the samples analyzed seemed to have a greater control upon the similarity between communities (Figure 3-2); although a detailed assembly of environmental (meta-) data would be useful in developing this hypothesis. This may be a product of the relatively constrained physiology of endemic hydrothermal vent bacterial microflora in light of varying environmental conditions across different vents. An additional explanation may be the high abundances of mesophilic vent bacteria in many diffuse flow/mesophilic habitats, which bias the composition of resulting clone libraries. A third explanation may be the limited resolution of the 16S rRNA in defining physiologically distinct populations of vent bacteria. A recent study of diffuse flow vent bacteria using “deep” pyrotag sequencing approaches revealed enormous degree of diversity at the subspecies level (Huber, Welch et al. 2007).

Within the Archaea, environmental factors appeared to play a larger role in shaping microbial community similarities (Figure 3-3). For example, low temperature environments (<50°C) clustered similarly. Likewise nascent hydrothermal chimneys and in situ incubation chambers (also presumed to be devoid of organic matter) clustered into similar groupings. These patterns may be the byproduct of bifurcating Archaea physiologies in the deep sea environment. In cool, benthic deep sea environments and the deep pelagic oceans there exists large populations of benthic Euryarcheota and Marine Group I Crenarchaeota, which are flushed through the vent environment during hydrothermal circulation. At the other end of the physiological spectrum, the most thermophilic organisms to date are found within the Archaea isolated from vent chimney

habitats. Thirdly, the Archaea features both obligately heterotrophic, fermentative metabolisms and are strict autotrophs. Often, these physiological and metabolic features are constrained to specific lineages (Madigan and Martinko 2006).

In summary, the community distributions amongst Archaea and Bacteria offer interesting trends which encourage further exploration. The data may be skewed by the limited resolution of the cloning and sequencing approach to find deep-lineages within the 16S rRNA gene. However, despite these limitations, there is intriguing evidence of vent bacterial populations being “jacks- of-all-trades,” occurring in a range of environmental niches, with a strong geographic overprint. The Archaea, on the other hands appear to be influenced by the energetic resources and environmental characteristics, which cause communities in like habitats to be more similar.

Implication for Autotrophy and Microbial Community Succession

The hydrothermal vent habitat, by nature, is a dynamic and heterogeneous environment. Niches are continually created, destroyed, renovated, are moved. Furthermore, obtaining detailed measurements of environmental characteristics pertinent to microbiological data within the chimney environment is challenging, to say the least. Comparative analyses of vent chimney populations within the confines of our limited environmental data sets provides insights into what may be factors controlling community composition in particular vent samples. The identity and occurrence of species which overlap between sites can then be queried in further detail, and integrated with manipulative experiments, both in the lab and field.

For example, the composition of microbial communities which initially colonize fresh, organic poor surfaces in the vent environment varies within the Bacteria, clustering into several

disparate groups. Within the Archaea, the communities which colonize nascent vents are more similar to one another, presumably are more constrained autotrophic community.

As the chimneys age and the structures developed strong thermal-chemical gradients and more organic matter is incorporated, the community similarities diversify. Within the archaeal communities, clustering is more influenced by environmental conditions such as temperature, whereas within the bacteria, the environmental component is less clear. Future studies targeting the organic matter composition, other gene loci including those involved specifically in carbon transformations, and greater sample resolution will aid in unraveling the complex pattern of heterogeneity and microbial community development in the vent chimney habitat.

CHAPTER IV: ABUNDANCE AND DISTRIBUTION OF TYPE II CALVIN CYCLE GENES WITHIN VENT CHIMNEY MICROBIAL POPULATIONS

INTRODUCTION

The Global Carbon Cycle

The production and degradation of carbon-bearing molecules is vital to the existence and proliferation of life on this planet. Carbon cycling through the biosphere consists of a balance between two primary components; the fixation of inorganic carbon to biomolecules through a process known as autotrophy, and the re-mineralization of organic compounds to carbon dioxide (CO₂) in a process known as respiration. Photosynthesis, autotrophy linked to light energy, the process by which green plants and cyanobacteria fix their carbon, has been extensively studied for decades (Bryant and Frigard 2006). In recent years, the magnitude and extent of a subsurface biosphere, subsistent upon chemical energy rather than light has become widely recognized (Bach, Edwards et al. 2006). However, the linkages between this so-called “dark energy biosphere” and photosynthetic life have not yet been elucidated, nor have tools been developed to study the inputs of “fixed” organic carbon quantitatively in such systems. Through this study the autotrophic Calvin Benson-Bassham (CBB) cycle in relation to the organic carbon content of hydrothermal vent chimney ecosystems will be investigated.

Environmental Constraints upon Autotrophy

The utilization of specific carbon fixation pathways in hydrothermal ecosystems is the culmination of the evolutionary history of microbial populations, sculpted by specific environmental constraints. Varying levels of red-ox active compounds, oxygen, and organic carbon concentrations specifically affect which organisms are present and their specific autotrophic metabolisms. Autotrophic biosynthesis is driven through red-ox reactions sustained

by chemical disequilibrium. High energetic costs are associated with the synthesis of biomolecules and for the transformation of surrounding carbon into usable forms. The highest costs are associated with the synthesis of autotrophy-related enzymes (Berg, Kockelkorn et al. 2010); therefore, environments with more ready-to-use or easily convertible carbon and large amounts of negative free energy will select for specific organisms and the pathways they participate in. Constraints on certain carbon assimilation pathways in hydrothermal chimney ecosystems are summarized below in Table 4-1.

Table 4-1: Constraints on carbon assimilation pathways (Berg, Kockelkorn et al. 2010)

Pathway	Oxygen Sensitivity	ATP Input
CBB	Facultative	7
rTCA	Microaerophilic	2
Acetyl - CoA	Obligate Anaerobic	~1

It can be seen that there are variations among how much energy is needed to “drive” each pathway and overall oxygen requirements. In the case of the CBB cycle, the most energetically “expensive” carbon fixation pathway, a requirement of seven ATPs is necessary for it to be operative. Most of the energy used is in the synthesis of Ribulose-1, 5-bisphosphate carboxylase oxygenase (RuBisCO), its key regulatory enzyme. This pathway is operative in both anaerobic and aerobic environments reserving its use to facultative and aerobic bacteria (Berg, Kockelkorn et al. 2010).

The Calvin-Benson-Bassham (CBB) Cycle

This study focused on investigating the CBB cycle, a pathway operative in both terrestrial and aquatic systems. The CBB cycle is thought to be the most prevalent carbon-fixation pathway on the planet (Badger and Bek 2008). Found in autotrophs, this pathway is composed of both phototrophs and chemotrophs with its exclusive use reserved towards bacteria and eukaryotic

species (Nakagawa and Takai 2008). Ribulose-1,5-bisphosphate carboxylase oxygenase (RuBisCO) serves as the key regulatory enzyme in this pathway, acting in catalyzing the carboxylation or oxygenation of RuBisCo with the addition of oxygen (O_2) or CO_2 (Nakagawa and Takai 2008). The CBB cycle uses a significant amount of RuBisCO enzyme and due to the number of species undergoing this process globally, it has been documented to be the most abundant protein on Earth (Badger and Bek 2008).

Different forms of RuBisCO

The key regulatory enzyme of the CBB cycle, RuBisCO, has at least four known forms besides the common variety found in chloroplasts of plants, algae, and cyanobacteria. The common Type I RuBisCO is made up of two distinct subunits. These subunits include both large (50-55 kDa) and small (12-18 kDa) subunits coded for in different locations within the cell. In eukaryotic organisms, the large catalytic subunit is coded within the chloroplast while the small subunit is coded in the nuclear genome. The dimerization of two L subunits (L_2) generates a catalytic center. The full quaternary structure of Type I RuBisCO has the sequence of L_8S_8 . In contrast, Type II RuBisCO is comprised solely of L subunits in the L_2 dimer form (Atomi 2002). There are many different forms of RuBisCO due to its imperfections as a catalyst. This enzyme is characterized as both an oxygenase and carboxylase. This means that this enzyme has low specificity for CO_2 due to the ability of O_2 to compete for binding sites on the enzyme (Badger and Bek 2008). Oxygen binding to RuBisCO lowers the efficiency of carbon fixation; this property added to its low turnover rate ($2-5 s^{-1}$) deems it as an imperfect catalyst. Due to these flaws, there are at least four unique RuBisCo species (Atomi 2002).

RuBisCO forms used in the CBB cycle are presumed to be selected for by overall CO_2 availability and O_2 prevalence. As mentioned previously, Form I is the most commonly-known

form of RuBisCO used primarily in the photic zone by green plants and cyanobacteria although its presence has been documented in deep-sea chemotrophs. Form II, focused upon in this study, is most prevalent in deep sea chemotrophs found in hydrothermal ecosystems. This form has a low affinity for CO₂ therefore this pathway is only found in CO₂-rich environments such as hydrothermal systems. Form III had been documented in sequencing analyses of deep-vent inhabiting hyperthermophilic Euryarchaeota but has not been thoroughly elucidated (Nakagawa and Takai 2008). A fourth type of RuBisCO is called RuBisCO-like protein which is not involved in the CBB cycle, but may have been an evolutionary precursor to modern day RuBisCO forms. These enzymes have been around before the evolution of the CBB cycle and have been found in the methionine salvage pathway in photosynthetic and non-photosynthetic Archaea and Bacteria (Ashida, Saito et al. 2003).

Evolutionary Significance

Autotrophic pathways in hydrothermal vent ecosystems are deeply-rooted in the evolutionary history of organisms on our planet. Some evidence for their antiquity is the oxygen sensitivity of key enzymes in autotrophic pathways, and the metal-rich environments in which they exist. On early Earth there was very low atmospheric oxygen available which necessitated that organisms develop metabolisms that functioned optimally in an anaerobic environment. Through the advent of oxygenic photosynthesis other autotrophic pathways came into existence that were either aerobic or aerotolerant (Thauer 2007). Hydrothermal ecosystems, having conditions conducive to lateral gene transfer, may have allowed the passing of functional genes amongst organisms (Brazelton and Baross 2009). This in theory could explain the existence and potential use of multiple pathways by organisms within hydrothermal ecosystems (Thauer 2007).

Reactions in hydrothermal environments are driven through red-ox reactions arising from catalytic metal sulfide surfaces. Many key enzymes, cofactors, and catalysts resemble these catalysts in autotrophic pathways with iron-sulfide reaction centers; therefore, early metabolism could have been driven through catalytic surfaces within the hydrothermal environment (Berg, Kockelkorn et al. 2010). Through elucidation of these pathways in organisms throughout hydrothermal systems, clues to the development of some of the earliest forms of life can be discovered. This can lead to ways to determine whether life can exist in other hydrothermal environments throughout Earth and throughout our solar system (Thauer, 2007).

OBJECTIVES

Analyses in this section were directed at determining the potential for autotrophic processes within hydrothermal systems investigated in this study. Organic carbon contents and carbon isotopic ratios were determined from sulfide vent samples to provide an idea about the presence of the CBB cycle based off of its specific isotopic signature, and provide a sense of the availability of organic carbon in the samples analyzed. Further studies led to genomic identification of the *cbbM* gene which codes for RuBisCO form II, a key regulatory enzyme within the CBB cycle found in deep hydrothermal ecosystems (Badger and Bek 2008; Hall, Mitchell et al. 2008). This was determined through the use of PCR - based assays to assess the presence of *cbbM* gene within hydrothermal vent populations. Genomic DNA extracts from hydrothermal samples were screened encompassing multiple chimneys throughout different gradients. Comparisons with taxonomic screens helped provide a link between overall diversity and functionality. Downstream analyses then aimed towards the quantification of relative *cbbM* gene abundances through the use of qPCR assays. Key objectives of these experiments are summarized below:

- 1.) Compare total organic carbon content and carbon isotope ratio geochemistry in chimney walls to biosignatures associated with the *cbbM* cycle
- 2.) Documenting the occurrence of the *cbbM* gene within vent chimney samples
- 3.) Quantifying the abundance of *cbbM* genes within the vent chimney habitat

HYPOTHESES

The hypotheses which were designed to address these objectives were:

- 1.) Carbon fractionation patterns correspond to the presence of the CBB cycle and the presence of *cbbM* genes.
- 2.) Genes for *cbbM* occur within the sulfide chimney habitat.
- 3.) The abundance of the *cbbM* gene is related to its position within the vent chimney gradient, with elevated abundances towards middle to exterior regions.

MATERIALS AND METHODS

Total Organic Carbon Analyses

Frozen sulfide chimney samples were pulverized, freeze dried, and sent to UC Santa Barbara Marine Analytical Lab for Elemental Analysis – Isotope Ratio Mass Spectrometry (EA-IRMS). Acidification was not necessary prior to analysis for basalt-hosted sulfide chimney samples due to their lack of carbonates and overall low pH (Xie, Wang et al. 2011). This method was used to determine the specific carbon fractionation pattern throughout the span of a hydrothermal chimney wall. Through mass spectrometry a $^{13}\text{CO}_2/^{12}\text{CO}_2$ ratio (R) is generated. This analysis uses combustion of natural compounds in order to provide a CO_2 medium for measurement. Values are generated as a $\delta^{13}\text{C}$ output which is equal to:

$$\delta^{13}\text{C} = ((\text{R-sample}/\text{R-standard})-1) \times 1000$$

In this equation, R is equal to the ratio of the heavy isotope (C^{13}) to the light isotope (C^{12}) in the sample or the standard. Units are reported either per mill or ‰. Lighter isotope, ^{12}C incorporation yields negative $\delta^{13}\text{C}$ values while heavier isotope, ^{13}C , incorporation yields positive values (O'Leary, 1988). Through the output of this analysis TOC concentrations within geological samples determine how much organic carbon “food” or organic biomass is available. Within hydrothermal systems, magmatic volatiles found within hydrothermal fluids have a carbon isotope CO_2 composition, $\delta^{13}\text{C}$, values ranging from -4 - -9 ‰ which are depleted in comparison to surrounding seawater CO_2 (bicarbonate) that has $\delta^{13}\text{C}$ equal to 0 ‰. Hydrothermal fluids alone have a range of $\delta^{13}\text{C}$ value from -3 - -11 ‰, these values overlap with magmatic volatiles' $\delta^{13}\text{C}$ values demonstrating volatile contribution to dissolved CO_2 in hydrothermal fluids. The combination of magmatic fluid upwelling and the presence of autotrophic pathways cause higher levels of organic carbon depletion in hydrothermal

environments (McCollom, 2008). It has been shown through isotopic studies of the Type II CBB pathway, that the isotopic fractionation pattern is -18‰ at its maximum (House, Schopf et al. 2003). Other studies have shown the endpoint fractionation pattern to be between the -35 to -25‰ (Berg, Kockelkorn et al. 2010). From CBB fractionation patterns deduced from previous studies, it is expected that the $\delta^{13}\text{C}$ values in these samples will range from -35‰ - -18‰ . A whole carbon budget is necessary to precisely constrain the system. In a study by Kato et al. 2010 the TOC concentrations within black smoker chimneys were determined from both active and inactive chimneys. Key findings of this study show that there was a direct correlation between TOC abundance and the activity of hydrothermal venting. Production of organics in these systems results directly from microbial activity. An example of this is found in inactive vents which have higher organic carbon concentrations (0.02-0.1 wt% TOC) than in active vents (0.015-0.02 wt%) due to encasement of biomass of the once active hydrothermal system (Kato, Takano et al. 2010).

PCR assays for the *cbbM* gene

The CBB cycle has previously been shown to be operative in deep-sea hydrothermal ecosystems (Badger and Bek 2008; Hall, Mitchell et al. 2008). This pathway relies on cascades of genes, enzymes, and biochemical pathways in order to ultimately fix inorganic carbon into biomass. Through the development of PCR-based assays to screen for the *cbbM* gene, key microorganisms participating in this cycle can be targeted. *cbbM* genes were amplified using a C1000 Thermal Cycler (Bio-Rad). A list of the primers (Invitrogen) and thermal cycling profiles used in *cbbM* gene amplification are shown below in Table 4-2.

Table 4-2: Primers used in *cbbM* PCR assays (Hall, Mitchell et al. 2008)

Gene	Primer Sequence	BP	Cycling Conditions
<i>cbbM</i>	cbbMf-ATCATCAARCCSAARCTSGGCTGCGTCCC	400	94°C 2 min; 30 cycles: 94°C 60 sec, 62°C
	cbbMr-MGAGGTGACSGCRCCGTGRCCRGCMCGRTG		60 sec, 72°C 60 sec, 72°C for 15 min

Each 5µl PCR reaction contained: 1 µl of template, 1× buffer, 0.2 mM dNTPs, 3µl 2% BSA, 2 µM forward and reverse primers, 2.5 U *Taq* polymerase, and molecular-grade water to make up the total volume of reaction. The *cbbMf/ cbbMr* primer set was used to amplify a 400 BP segment of the *cbbM* gene coding for RuBisCO form II. The results for all functional gene screens were visualized on 2% agarose gels ran at 70V. A *cbbM* clone was used as a positive control for these assays. An image of a positive *cbbM* screen is pictured below in Figure 4-1.

Positive Control

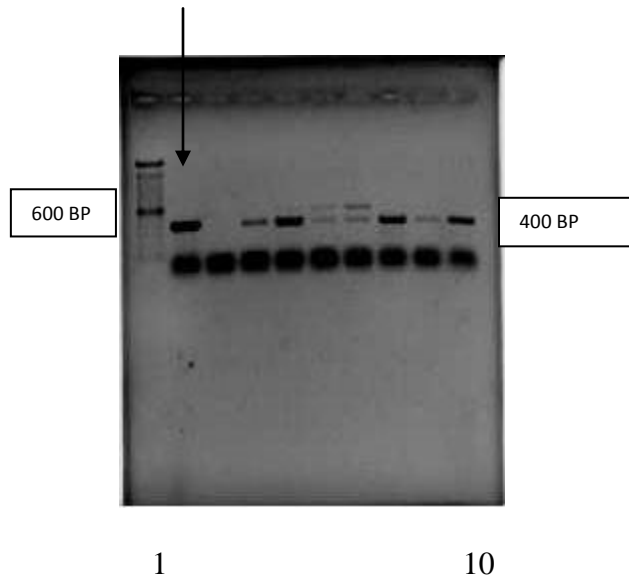


Figure 4-1: Gel image of a positive *cbbM* functional gene screen

A 100 BP ladder (lane one) was used as the size standard. Positive and negative controls are found on lanes 2 and 3 respectively. Lanes 4, 5, 8, 9, 10 all contain specific *cbbM* PCR products, with lanes 6, 7 having non-specific amplification of *cbbM* (samples were not used in analysis).

***cbbM* qPCR Analyses**

Once the presence of the *cbbM* gene was determined, qPCR assays were performed to determine the abundance of the *cbbM* gene. These assays were conducted on the CFX96 Real-Time PCR Detection System (Bio-Rad) similar to archaeal and bacterial qPCR analyses. Both methods had the same PCR reagent concentrations utilizing the SYBRgreen molecular probe (see Chapter II methods), but with different primers (Invitrogen) and cycling conditions. The primers and respective cycling conditions used in these analyses are shown below in Table 4-3.

Table 4-3: Primers used in *cbbM* qPCR assays

Gene	Primer Sequence	BP	Cycling Conditions
<i>cbbM</i>	cbbMF-ATCATCAARCCSAARCTSGGCTGCGTCCC	400	98°C 2 m; 40 cycles:
	cbbMR-MGAGGTGACSGCRCCGTGRCCRGCMCGRTG		98°C 2 s, 60°C 2 s

Samples were run in triplicate. Quantification of *cbbM* genes per sample was determined through the use of pure plasmid DNA standards from a *cbbM* positive clone. Standards were run in triplicate generating a standard curves with an r^2 value equal to 0.930 pictured below in Figure 4-2.

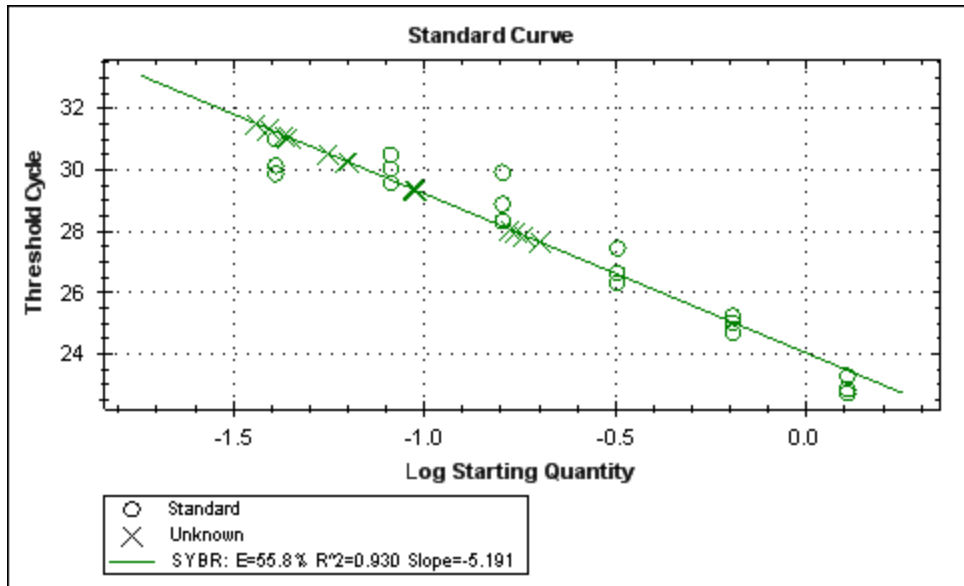


Figure 4-2: Standard curve used in *cbbM* qPCR gene quantification

The detection limits for *cbbM* amplification were from 6.11E4 – 3.91E8 *cbbM* gene copies/ g sample (0.02 pg/μl -128 pg/μl standard concentration). These values were calculated for 3 grams sulfide yielding 50 μl of DNA extract. Melt curve analyses were performed at the completion of each run to ensure peaks arising from a single PCR product. The melt curve generated through these analyses is shown below in Figure 4-3.

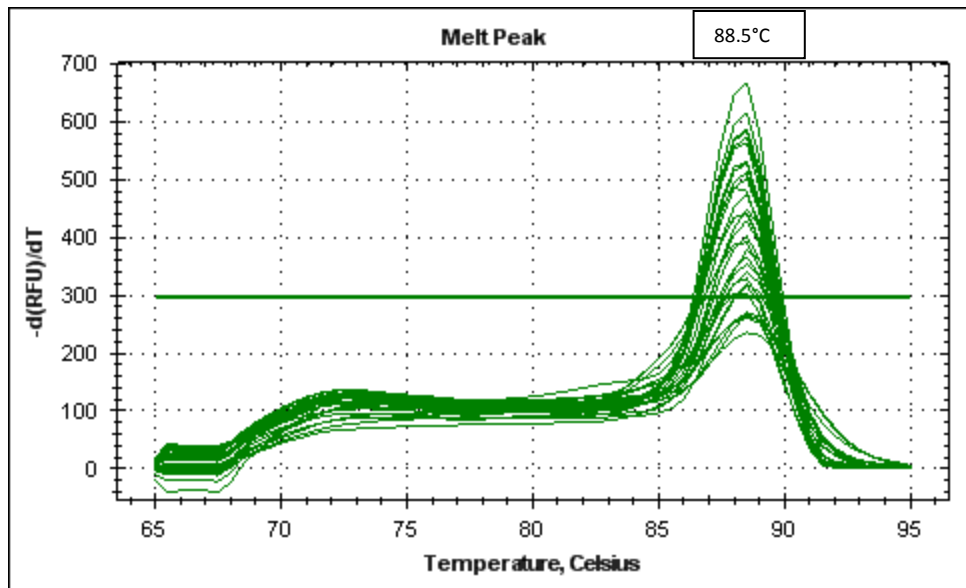


Figure 4-3: Melt curve at completion of *cbbM* qPCR run

T-tests were performed to determine the statistical significance of results.

RESULTS

EA-IRMS Analysis

EA-IRMS analyses aimed towards quantifying usable stores of inorganic and organic carbon for its incorporation into biomass by microorganisms. The results of carbon analyses for the chimney Finn are displayed below in Figure 4-4.

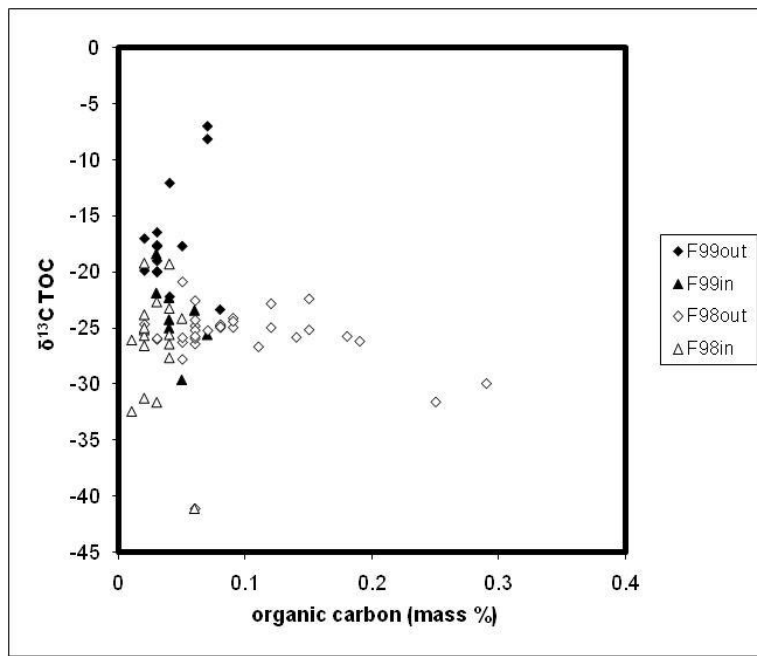


Figure 4-4: Results from EA-IRMS analysis of the sulfide chimney Finn

This figure shows the fractionation ratio, $\delta^{13}\text{C}$, between ^{12}C and ^{13}C versus the percent mass of organic carbon in the analyzed samples. Four types of samples were analyzed, all from the hydrothermal vent Finn: Finn99 is a younger, active sample, while Finn98 is from a settled mature chimney. Overall $\delta^{13}\text{C}$ values from these two samples are negative indicating higher ^{12}C incorporation into biomass (O'Leary, 1988). Results also indicate key $\delta^{13}\text{C}$ values are indicative of autotrophic processes with most samples having $\delta^{13}\text{C}$ values around the -35‰ to -25‰ range indicative of the CBB cycle fractionation pattern (Berg, Kockelkorn et al. 2010). These

fractionation patterns are found in both F99 and F98 chimneys indicating that these processes occur during active and inactive venting processes. The F98 out sample has higher organic carbon percentages showing that more established chimneys have more exterior organic carbon which can be used by heterotrophs. This could indicate that this organic carbon is produced over time through autotrophic processes. However, an accurate determination will entail confirming that *cbbM* genes are being expressed and accurately quantifying the sources and sinks of carbon through these systems (*e.g.* developing a total carbon budget).

***cbbM* Gene Assays**

To help link functionality to taxonomy, *cbbM* screens were compared to corresponding taxonomic screens. These results are summarized below in Table 4-4.

Table 4-4: Key findings of *cbbM* gene assays

Samples	Chimney	Zone	Bac 16s	Arch 16s	<i>cbbM</i>
A: F-AT	Finn	ext	x	x	x
G3FeSi	Finn	ext	x	x	x
FeSi	Finn	ext	x	x	x
FeSi 6/25/01	Finn	ext	x	x	x
FeSi 8/20	Finn	ext		x	x
FG3Fe	Finn	ext	x		x
B:FZ2B	Finn	mid	x	x	x
Fpyr	Finn	mid	x	x	x
Fpyr 4/23/01	Finn	mid	x	x	x
E: MEF R-002 (adj)	n/a	bkgd	x	x	x

These results show the presence of the *cbbM* gene throughout hydrothermal gradients found primarily in middle to exterior chimney gradients. Taxonomic comparison shows that this gene was found throughout both positive bacterial and archaeal-positive samples.

***cbbM* qPCR Analyses**

qPCR analyses were performed to determine *cbbM* gene abundances through a variety of chimney gradients. A summary of data collected from *cbbM* qPCR analysis is shown below in Table 4-5.

Table 4-5: *cbbM* qPCR data

Sample	Chimney	Gradient	<i>cbbM</i> gene copies/ g sample	error
15 - G2pyr-cpy	Finn	Int	2.93E+06	3.36E+06
13: F-G4pyrL(1 in cpy)	Finn	Int	3.40E+02	4.29E+02
Fpyr	Finn	Mid	3.24E+05	1.19E+03
B: FZ2B	Finn	Mid	2.19E+07	1.39E+06
34- FinnSmokerMid	Finn	Mid	2.45E+07	3.33E+06
A: F-AT	Finn	Ext	2.06E+06	8.31E+05
G3FeSi	Finn	Ext	2.95E+06	1.87E+05
G: Hulk Piece 1	Finn	Ext	1.68E+07	1.50E+06
C: MEF R-003	MEF	Bkgd	3.81E+06	3.17E+05
E: MEF R-002 (tube)	MEF	Bkgd	7.67E+07	1.15E+07
D: MEF R-002 (away)	MEF	Bkgd	2.05E+04	3.15E+03

This chart displays gene copies per gram of extracted sample and the extraction data used to generate the final quantity. Samples analyzed were mainly from the sulfide chimney Finn, while others were background samples from the Main Endeavour Field. A chart summary of the results from this study is shown below in Figure 4-5.

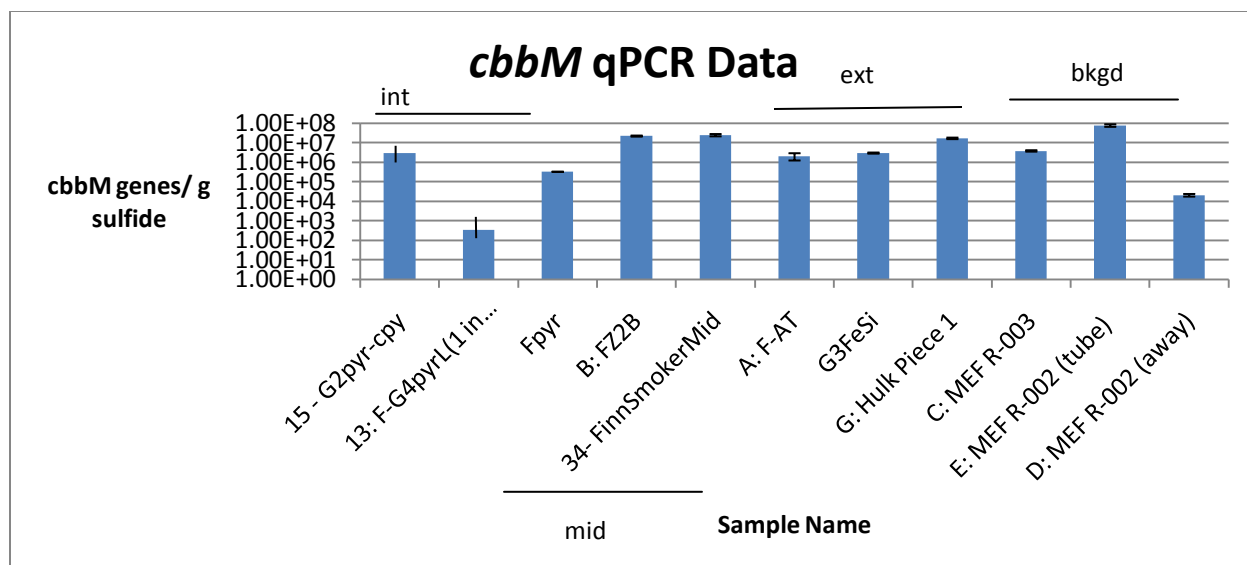


Figure 4-5: Results summary from *cbbM* qPCR

Upon interpretation, it can be seen that cell abundances vary between chimneys and gradients from both the MEF and Mothra field. A major trend points out that there was a significantly larger proportion ($p = 0.05$) of *cbbM* genes in exterior-to-middle chimney zones as opposed to interior chimney zones.

In order to gain an overall estimate of the taxonomic contribution to these pathways, the relative percentages of *cbbM* genes out of total taxonomic gene abundance numbers were calculated. Pictured below in Table 4-6 is data for representative samples of Finn exterior and middle chimney gradients.

Table 4-6: *cbbM* gene percentages among taxonomic gene abundances

Sample	Gradient	Bac 16S	<i>cbbM</i>	%16S	Significance (p-value)
B: FZ2B	Mid	2.95E+07	2.19E+07	74%	0.05
G3FeSi	Ext	7.92E+07	2.95E+06	4%	0.25

It is shown in the table above that within the middle gradient of the Finn sulfide chimney a significant proportion ($p = 0.05$) of *cbbM* genes corresponds to bacteria 16S rRNA genes. This

can suggest that *cbbM* may be found within a potentially significant percent of the bacteria population in middle chimney gradients.

DISCUSSION

Analyses in this section aimed towards showing that the CBB cycle was present within hydrothermal chimneys through both geochemical and genomic analyses. Initial geochemical analyses were used to address specific carbon fractionation patterns associated throughout the length of the chimneys investigated in this study. Further genomic approaches worked towards classifying the presence and overall abundance of the *cbbM* gene coding for the key regulatory enzyme RuBisCO in the CBB cycle. Genomic results from both functional and taxonomic gene assays were then compared providing a link between overall functionality and diversity within these ecosystems.

EA-IRMS analyses were used to quantify carbon fractionation patterns and overall organic carbon abundances throughout the length of a hydrothermal chimney. Upon quantification, it appeared that the $\delta^{13}\text{C}$ fractionation patterns spanning throughout chimney length were mainly characteristic of the CBB cycle. CBB fractionation patterns were negative indicating high incorporation of ^{12}C into biomass showing active autotrophic processes (O'Leary 1988). Upon examination of organic carbon percentages, it was shown that older chimneys have higher organic carbon content than newly-formed chimneys. This is consistent with the current theory that newly-formed vent habitats have predominantly autotrophic species, but over time organic biomass produced through autotrophic pathways becomes a more prominent portion of the structure (Schrenk, Kelley et al. 2003; McCliment, Voglesonger et al. 2006).

Genomic analyses to confirm the presence and determine the overall abundance of the *cbbM* gene were also conducted. PCR assays showed the *cbbM* gene was found throughout hydrothermal gradients. This gene was especially prevalent throughout the lower temperature, middle to exterior chimney gradients. In these regions there is an especially high amount of

bacterial species which correspond to the key CBB participants (Schrenk, Kelley et al. 2003; Badger and Bek 2008). Studies have shown that the CBB pathway is found in predominately *Gammproteobacteria* found in both free-living and symbiotic bacteria residing within tubeworms and mollusks found on and surrounding the exterior of hydrothermal chimneys (Nakagawa and Takai 2008).

Main samples investigated in this study were found throughout different Finn gradients and bulk samples from the MEF. Even though the *cbbM* gene was found throughout middle and exterior chimney gradients, *cbbM* gene abundances were significantly elevated within middle chimney gradients. Upon comparison with taxonomic gene assays, *cbbM* constituted a significant proportion of middle gradient bacterial 16S rRNA genes. It has been shown thermodynamically that there is significant energy for diverse metabolisms in middle chimney gradients due to the large extent of fluid mixing disequilibrium feeding the metabolisms of bacteria (McCollum and Shock 1997).

In summary, it was shown that geochemical and genomic signatures indicate the presence of the CBB cycle throughout hydrothermal samples. Genomic screens for the *cbbM* gene show its presence in middle to exterior chimney portions. Upon looking at qPCR data, it was shown that *cbbM* gene abundances make up a larger percentage of bacteria genes found in hydrothermal systems particularly in middle gradients. These data provide support for the CBB cycle's evidence in both CBB symbionts in the chimney exterior gradients and free-living bacteria throughout chimney middle gradients.

CHAPTER V: PHYLOGENETIC ANALYSIS OF THE TYPE II CALVIN BENSON-BASSHAM PATHWAY FROM VENT CHIMNEYS

INTRODUCTION

Two primary factors play a role in determining which metabolic pathways organisms conduct. Environmental controls force organisms to utilize pathways based off of ecological stressors, but over time become hard-wired into the evolutionary history embedded within the genomes of these organisms. The Calvin Benson-Bassham (CBB) cycle may be the most energetically-taxing autotrophic pathway, but this pathway still remains one of the most prevalent pathways in hydrothermal environments, especially those at interfacial environments with mixtures of hydrothermal fluids and seawater. Through the course of evolutionary history many genes have been passed along either directly or horizontally, leading to metabolic diversity (Berg, Kockelkorn et al. 2010). Understanding this diversity provides a means to further understand the phylogeny and ecology of autotrophy.

Approaches to Study the Type II Calvin Cycle

The focus of this thesis is on the CBB Cycle's use of RuBisCO Form II to fix CO₂ in hydrothermal environments. Studies aimed towards determining the distribution and phylogeny of the Type II Calvin Cycle work towards linking both the presence of the functional genes to the diversity of organisms within specific ecosystems. Phylogenetic studies of the Type II CBB Cycle have been conducted within deep-sea microbial endosymbionts, hydrothermal fluids, and chimney structures. Earlier studies have identified bacterial genera such as *Rhodospirillum*, *Rhodobacter*, *Thiobacillus*, and *Hydrogenovibrio* which harbor the CBB pathway (Atomi 2002). Later findings were able to find some Archaea harboring Form II RuBisCO genes but with inoperative pathways (Atomi 2002). Classical studies used cloning, and downstream clustering

and phylogenetic analyses to identify different relationships between organisms in these systems. Recent studies such as the one performed by Wang and colleagues, paired traditional cloning with GeoChip or pyrosequencing analyses identifying key functional genes and taxonomy within a hydrothermal community (Wang, Zhou et al. 2009). Wang's study in particular looked at newly formed chimney structures at the Juan de Fuca Ridge (JdFR), identifying characteristic CBB cycle genes. Gene probes for Form I and II of RuBisCO genes were used to identify functional genes within the community. Form II RuBisCO genes were found on the exterior chimney region in tubeworm symbionts. Microbial communities interior to the structures had 20% *Proteobacteria* species harboring the Form II RuBisCO gene (Wang, Zhou et al. 2009). In addition to GeoChip analyses, 454 pyrosequencing have allowed comparative metagenomic studies such as performed by Xie et al, 2011. Through this study specific gene sequences pertinent to both autotrophic pathways and metabolisms were collected. The CBB cycle was reconstructed based upon gene sequences obtained. These data were paired with metabolic genes which determined that this pathway is likely fueled by sulfur oxidation coupled to nitrate reduction. Through these studies one has the potential to deduce metabolic potentials and adaptation strategies of microorganisms within select communities (Xie, Wang et al. 2011). With the advent of next generation sequencing technologies paired with traditional microbial ecology approaches, linkages between functionality and taxonomy can be elucidated.

Key Type II Calvin Cycle Participants

Through a number of phylogenetic studies, the key functional genes for the Type II Calvin Cycle were found mainly in mesophilic chemoautotrophs. These species include endosymbiotic α , β , and γ -*Proteobacteria* (Nakagawa and Takai 2008). RuBisCO has a very low affinity for CO₂ therefore requiring a large amount to be operative. Most participants are found

in anaerobic or facultative environments with high levels of CO₂ (Badger and Bek 2008). Due to the facultative nature of some Type II Calvin Cycle participants, they contain both Type I and II RuBisCOs allowing them to utilize the CBB cycle at lower CO₂ levels and elevated O₂ levels. On the other hand, anaerobic participants only use RuBisCO Form II confining their CBB cycle to high CO₂ conditions (Elsaied and Naganuma 2001; Badger and Bek 2008). Based upon our current state of knowledge about the taxonomic distribution of the Type II CBB, this pathway is indicative of the presence of anaerobic, mesophilic chemoautotrophs. Even though some microorganisms are completely reliant upon the CBB cycle, it has also been found that endosymbionts in vent environments harbor diverse autotrophic processes across a variety of niches fueled through multiple energy utilization pathways. Endo- and epi-symbiotic metabolic diversity is thought to be associated with geochemical constraints. Less information is known about the biogeography of free-living microorganisms in vent environments (Nakagawa and Takai 2008). Understanding autotrophic diversity within vent environments and the factors which play a role in their occurrence will provide a better picture of the extent of primary production in deep-sea vent ecosystems.

Evolutionary Significance of the Type II Calvin Cycle

As mentioned previously, Type II of the CBB cycle utilizes an O₂ sensitive form of RuBisCO. It is thought that this may be a derivative of the common ancestral form of RuBisCO due to its confinement to the high CO₂, low O₂ environment (Elsaied and Naganuma 2001). Early Earth conditions, prior to the Great Oxidation Event, had little to no O₂, or oxygen distributions which were highly localized (Thauer 2007). It can be inferred that metabolic pathways utilized could not have oxygen as an electron acceptor due to the high levels of CO₂ in the atmosphere (Thauer 2007). Autotrophic enzymes with oxygen sensitivity or intolerance could represent some

of the earliest pathways on the planet. Specifically this can be seen through the evolution of RuBisCO in CBB cycle participants. It has been observed that the more highly evolved the species, the higher the affinity RuBisCO has for CO₂. This can be seen in increasing RuBisCO CO₂ affinities from bacteria to cyanobacteria to higher plants (Jordan and Ogren 1983). In higher species, the evolution of RuBisCO to have a higher affinity for CO₂ provides a means to cope with high O₂ levels in the atmosphere. Through understanding how different forms of RuBisCO enzymes are distributed throughout hydrothermal communities, evolutionary clues can be determined about the origin of autotrophic pathways and their relationship to environmental factors (Elsaied and Naganuma 2001).

OBJECTIVES

The overall diversity of the Type II CBB Cycle was determined through phylogenetic analysis of *cbbM* gene sequences and their respective protein translations. The *cbbM* gene codes for RuBisCO Form II prevalent in the CBB cycle in deep sea hydrothermal environments. This study served as a comparison between the distributions of the *cbbM* gene amongst two hydrothermal chimney ecosystems. The phylogenetic trees between DNA and protein sequences were also compared to look for any incongruities in their distributions. The culmination of these studies aim towards fulfilling the following objectives:

- 1.) To clone representative *cbbM*-amplifying samples and conduct phylogenetic analyses to examine overall gene and protein diversity.
- 2.) To observe the diversity of the *cbbM* gene and protein sequences within different hydrothermal chimney environments.

HYPOTHESES

Through conducting this phylogenetic study, I hypothesized that:

- 1.) *cbbM* sequences from the same chimney environment will be most similar to each other.
- 2.) The phylogeny of *cbbM* sequences will be congruent with the phylogeny of 16S rRNA genes.

MATERIALS AND METHODS

Cloning *cbbM* Sequences and Exporting Files

A subset of successfully-amplifying *cbbM* samples from Chapter 4 was cloned in order to assess the overall diversity of the *cbbM* throughout select hydrothermal ecosystems. A list of samples cloned in this study is shown below in Table 5-1.

Table 5-1: *cbbM* positive samples cloned for phylogenetic analysis

Clones	Samples	Chimney	Gradient	Field
C4	A: F-AT	Finn	ext	Mothra
C5	B:FZ2B	Finn	mid	Mothra
C-3	G3FeSi	Finn	ext	Mothra
C7	FeSi	Finn	ext	Mothra
C-1	FeSi 6/25/01	Finn	ext	Mothra
Hk2	Hulk Incubator	Hulk	Placed within chimney	MEF
C6	E: MEF R-002 (adj)	n/a	bkgd	MEF

Most samples are from the sulfide Finn, primarily from exterior gradients with one background sample from the Main Endeavour Field. Clones from an incubator placed in the chimney Hulk were used to compare one chimney ecosystem to another. Sequences were compiled and sent to us from colleagues at the University of Washington (c/o D.S. Kelley). Prior to beginning cloning procedures, *cbbM* PCR was performed on the samples and checked for positive amplification (see Chapter 4 methods). To obtain high quantities of pure DNA for input into cloning reactions, positive PCR reactions were performed in triplicate, pooled, and purified (QiaQuick PCR Purification Kit, Qiagen). The TOPO-TA cloning kit (Invitrogen) was used with either a pCR2.1 or pCR4 vector (Invitrogen). Depending on what vector was used, Top10F' (pCR2.1) or Top10 (pCR4) competent *E. coli* cells (Invitrogen) were transformed with the *cbbM* 400 BP gene

amplicon. Clones containing the insert were grown on LB/AMP plates (50 µg/ml AMP) overnight and were picked and transferred to clone libraries.

Prior to sequencing, clones were checked for the insert using vector-specific primers. Plasmids were incubated at 37°C for 1 hour at 225 rpm in LB/AMP broth. A PCR reaction was performed with M13 primers to determine if the correct-sized fragment (~500 BP) was produced. The 50 µl M13 PCR reaction contained: 1 µl template, 1× buffer, 0.4 mM dNTPs, 0.8 µM forward and reverse primers, 1.625 U *Taq* polymerase, and molecular biology-grade water to make up the total volume of reaction. Primers (Invitrogen) used to test for the M13 insert are shown below in Table 5-2.

Table 5-2: Primers used in M13 PCR of cloned plasmid DNA

Primers	Gene Target	Primer Sequence (5'-3')	Amplification Conditions
M13 F	pCR 2.1/ 4.0 plasmid	GTAAAACGACGGCCAG	94°C 2 min; 30 cycles: 94°C 30 sec, 54°C
M13 R	pCR2.1/4.0 plasmid	CAGGAAACAGCTATGAC	45 sec, 72°C 2 min; 72°C 10 min.

Plasmids with positive M13 PCRs were incubated overnight prior to miniprep purification. Miniprep was performed to extract and purify plasmid DNA for sequencing using the QIAprep Spin Miniprep Kit (Qiagen). Clones were sequenced at the Core Genomics Facility at East Carolina University (c/o Denise Mayer) using M13 forward and reverse primers.

Forward and reverse sequence reads of approximately 400 base pairs were assembled as contigs and edited using Sequencher 4.9 program (Gene Codes). Once contigs were fully assembled, BLASTn (NCBI) was used to blast DNA sequences against non-redundant protein sequences within the bacteria database to determine if the *cbbM* gene cloned coded for RuBisCO Form II. All sequences used in this study were successfully BLAST-ed for the *cbbM* gene.

Consensus sequences from all contigs were exported and put into FASTA format for downstream computational analyses.

BLASTx was then used to compile protein sequences for all contigs. This was performed by looking at protein sequences from top blast hits and determining which reading frame the protein was translated in. If there was a negative reading frame, DNA sequences were transformed to their reverse complement and exported in that form using Sequencher. The translations for each contig from each specific reading frame were exported. Protein files were then transformed into FASTA format for downstream computational analysis.

Phylogenetic Analysis

DNA and protein sequences were first edited using both Bioedit Sequence Alignment Editor (Tom Hall, Ibis Biosciences) and SeaView (Goury, Guindon et al. 2010) programs. Once edited a multiple alignment was performed on both sets of sequences using the ClustalX2 program (EMBL-EBI).

To provide a means of sequence comparison, phylogenetic trees were produced through Clustal X2 using a neighbor-joining, bootstrap analysis for both DNA and protein sequences. Trees were visualized and modified using TreeView software (Roderic D. M. Page, Taxonomy and Systematics at Glasgow) and Adobe Illustrator.

RESULTS

The results of this study led to the production of two different phylogenetic trees containing both *cbbM* DNA and translated protein sequences respectively. Sequences were compiled from two hydrothermal vent chimneys, Finn and Hulk, as well as a background benthic deep-sea sample. Phylogenetic analyses allowed the comparison of sequences amongst chimney ecosystems. Top BLAST hits to specific sequences were included in phylogenetic analysis to provide a taxonomic comparison.

BLASTn

The results from performing BLASTn searches on *cbbM* DNA sequences are shown below in Table 5-3.

Table 5-3: Top BLASTn matches to *ccbM* clone sequences in GenBank; all sequences were 329 BP in length.

Clone ID	DNA ACN	Identity	Location	Sample	Proteo.
hulkinc_cbbM18, 29	AB629659	88%	Suiyo Seamount	rock	?
FinnExt_C4_14	EU926520	79%	tar contaminated aquifer	?	beta
FinnExt_C4_12	AY431001	78%	P Vent, EPR	?	beta
FinnExt_C4_20	EU926570	79%	tar contaminated aquifer	?	beta
FinnMid_C5_47	FJ640838	99%	Mothra chimney	rock	alpha
hulkinc_cbbM2, 12, 27	HQ675079.1	78%	Ocean	?	gamma
hulkinc_cbbM4, 23	FN659777.1	81%	Epibiotic HV Community	?	uncul.
hulkinc_cbbM1, 16, 25	DQ272535	76%	pure culture, <i>T. crunogena</i>	culture	gamma
hulkinc_cbbM13	AB174758.1	87%	Mariana, W. Pacific Arc	plume	uncul.
hulkinc_cbbM33	AM883190.1	80%	Arctic Cold Seep	tube.	?
hulkinc_cbbM19	FM165440.1	87%	Med. Cold Seep	tube.	?
hulkinc_cbbM26, 31	FN562918.1	76%	Logatchev field	mussel	?
hulkinc_cbbM30	FM165442.1	76%	Med. Cold Seep	tube.	?
MEF_C6_17	HQ675084.1	75%	Ocean	?	gamma
FinnExt_C1_1, 3, 12, 32, 33	HQ675084.1	75%	Ocean	?	gamma
FinnExt_C1_24, 26	HQ675075.1	75%	Ocean	?	gamma
FinnExt_c4_10, 15	DQ232898.1	82%	Guaymas Basin	tube.	?
FinnExt_c4_22	AY099399.1	76%	Groundwater, aquifer	water	gamma
FinnExt_c4_1, 2	AB629666.1	77%	Deep Sea Vent	?	?
FinnExt_c4_6, 16	HQ638675.1	86%	Magnetotactic bacteria	culture	gamma
FinnExt_c1_15	FJ629373.1	87%	Magnetotactic bacteria	culture	alpha
FinnExt_c7_23	GQ888606.1	88%	Hypersaline Lake	sed.	gamma
FinnExt_c1_31	GQ888606.1	84%	Hypersaline Lake	Sed.	gamma
FinnExt_c1_3, 4, 34	AY450592.1	78%	Magnetotactic bacteria	culture	alpha
FinnExt_c3_1, 6, 7, 17, 21	AY450592.1	79%	Magnetotactic bacteria	culture	alpha
FinnMid_c5_10, 17, 19, 21, 26	AY450592.1	79%	Magnetotactic bacteria	culture	alpha
FinnMid_C5_27, 28, 31, 42,43	AY450592.1	78%	Magnetotactic bacteria	culture	alpha
FinnMid_c5_44, 45, 48	AY450592.1	79%	Magnetotactic bacteria	culture	alpha
FinnMid_c5_15, 25	GQ888611.1	83%	Hypersaline Lake	sed.	gamma
FinnExt_c1_27	GQ888611.1	82%	Hypersaline Lake	sed.	gamma

cbbM DNA Sequences

A simplified version of the neighbor-joining phylogenetic tree produced from aligned DNA sequences is shown in Figure 5-1.

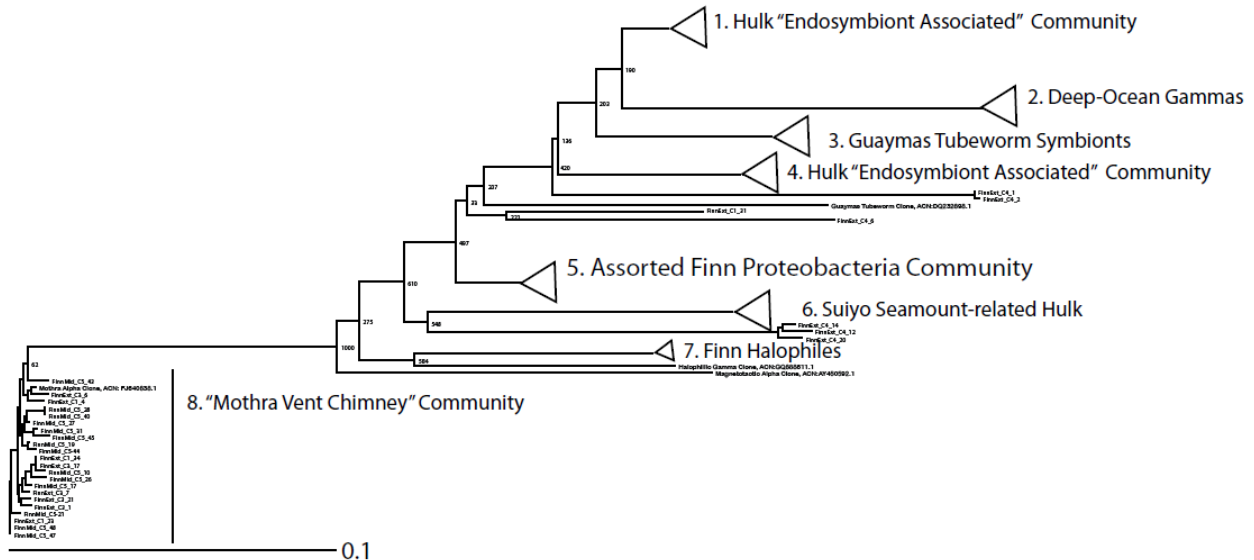


Figure 5-1: Simplified complete neighbor-joining phylogenetic tree of *cbbM* DNA sequences.

This tree contains sequences from both Finn and Hulk along with top BLASTn hits. Alignments and trees were generated using the ClustalX2 software.

The phylogenetic tree of *cbbM* gene sequences designates key clusters of organisms grouped together based on their most similar BLAST sequences. It can be seen that there is significant diversity amongst *cbbM* participating species found throughout Finn and Hulk vent chimney ecosystems. It can also be seen that Hulk sequences form distinct groupings in relation to Finn where there is vast diversity among its sequences as well. Both top and bottom-branching regions were examined in detail to gain an overall understanding of the microbial diversity in relation to the functional diversity of *cbbM*. The top branch of the *cbbM* DNA phylogenetic tree is shown below in Figure 5-2.

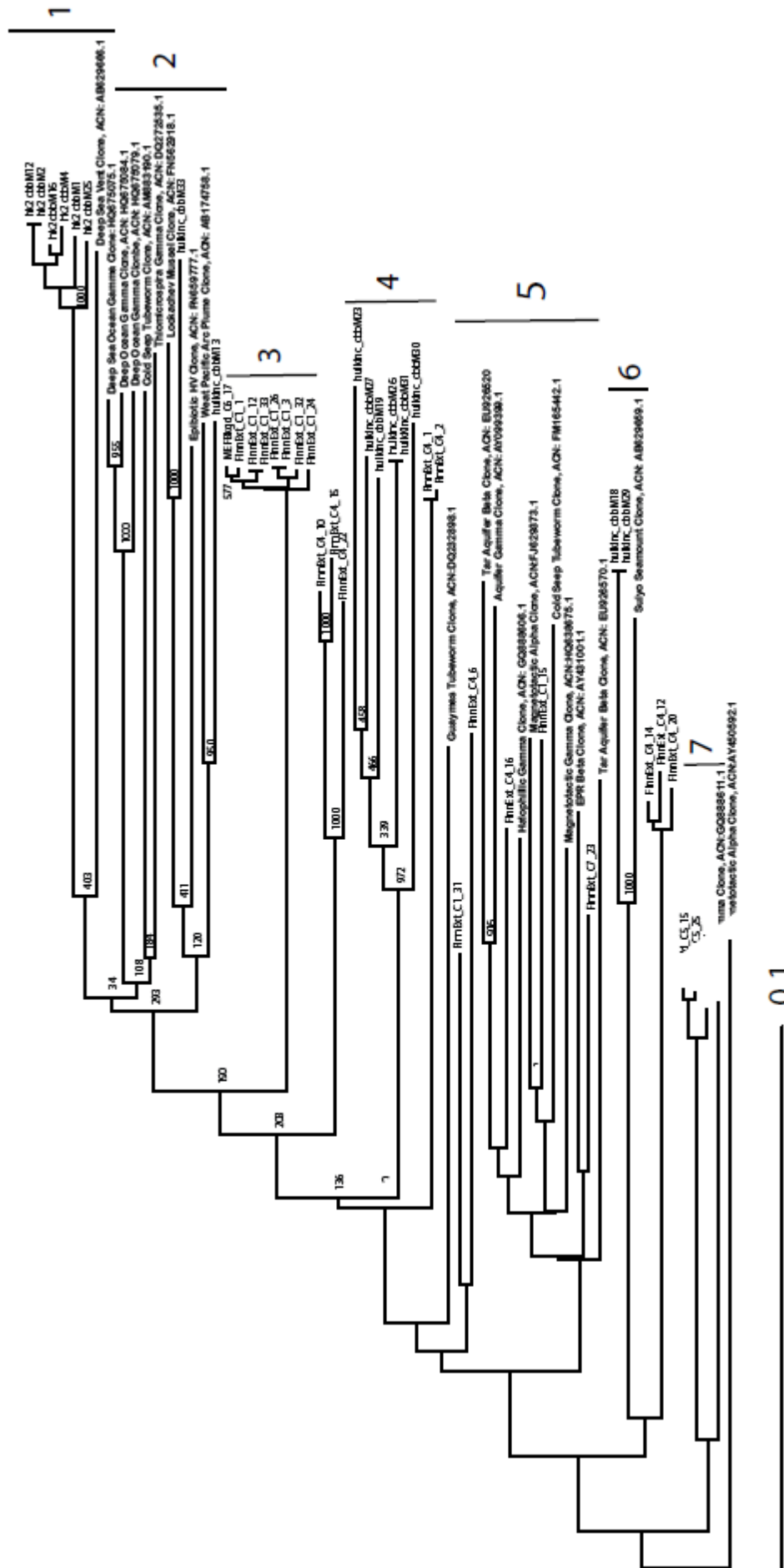


Figure 5-2: The detailed upper branch of the phylogenetic tree of cbbM DNA sequences.

The tree shows a detailed account of sequences contained within the upper branch of the *cbbM* DNA phylogenetic tree. Distinct clusters of DNA sequences are numbered based on the groupings designated in Figure 5-1. Clusters 1, 2, 4, and 6 are all from the chimney Hulk and upon examination it can be seen that these sequences are most related to distinct groupings of free-living gamma *Proteobacteria*, submarine volcano inhabitants, and a variety of endosymbiont bacteria. This shows that there is a significant amount of diversity among Hulk *cbbM* participants encompassing a variety of ecological niches throughout the hydrothermal chimney ecosystem.

In addition to the diversity of Hulk microbial communities, a high level of diversity was also captured among Finn *cbbM* sequences. Distinct clusters of Finn include 3, 5, and 7 encompassing a multitude of different *cbbM* participants related to various forms of *Proteobacteria* including symbionts, and halophiles. *Proteobacteria* found within the Finn chimney include gamma, alpha, and beta forms related to microflora throughout vent ecosystems.

The bottom branch includes a diverse cluster of DNA sequences shown below in Figure 5-3 classified as the “Mothra Vent Chimney” community.

8. “Mothra Vent Chimney” Community

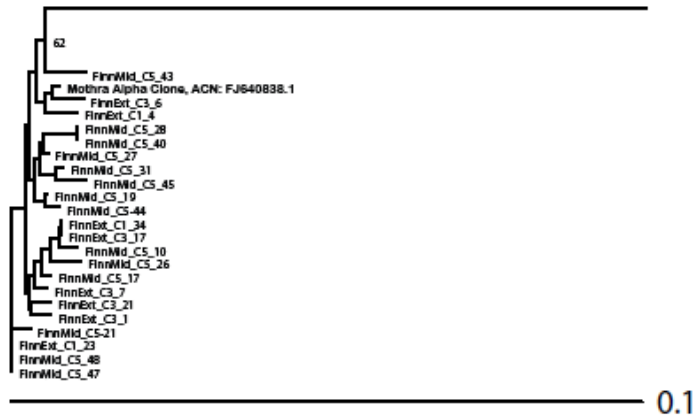


Figure 5-3: The bottom-branch, “Mothra Vent Chimney” Community, DNA sequence cluster from the Finn chimney ecosystem.

This cluster is diverse because it contains sequences throughout the middle and exterior portions of Finn from a variety of different clone libraries. The closest-related BLAST hit among sequences was an alpha *Proteobacteria* clone from the Mothra hydrothermal field, obtained in the previous study by Xie, et al.

Protein Sequences

A neighbor-joining phylogenetic tree was also generated from protein sequences translated from *cbbM* clones, a simplified version of this tree is shown below in Figure 5-4.

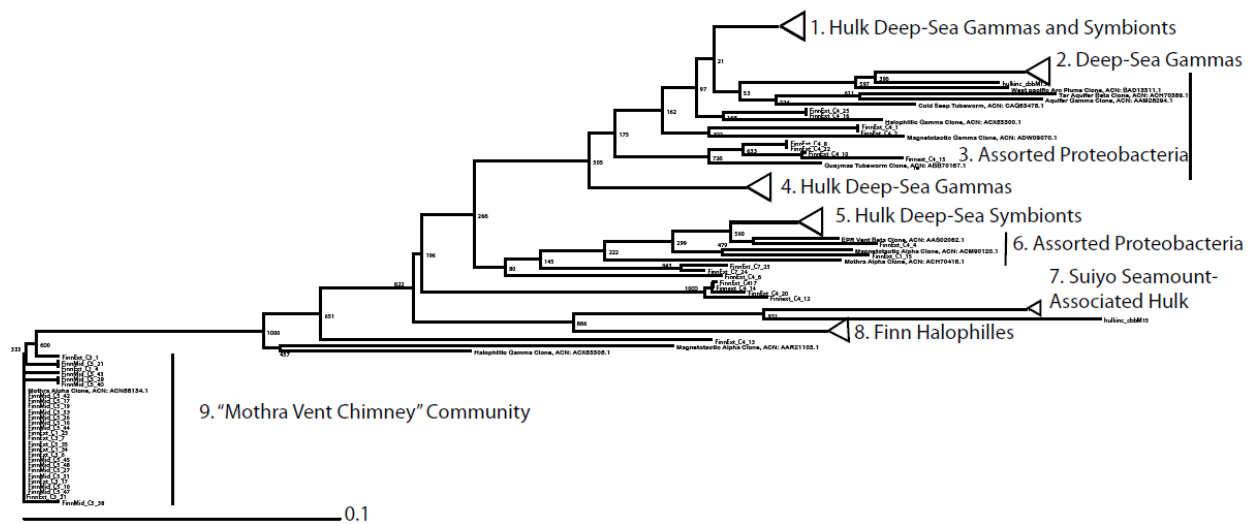


Figure 5-4: Simplified complete neighbor-joining phylogenetic tree of *cbbM* protein sequences. This tree contains sequences from both Finn and Hulk along with top BLASTn hits. Alignments and trees were generated using the ClustalX2 software.

Upon comparison with *cbbM* DNA sequences, there appears to be similar tree topology demonstrating that there is a high level of diversity on the protein level. Among tree clusters there are similar groupings of organisms representing different taxonomic groups among the *Proteobacteria* class.

DISCUSSION

Hydrothermal systems are extreme environments with complex chemical and physical conditions selecting for the prevalence of unique inhabitants with adaptations stemming through the use of specific autotrophic metabolisms. In this study, samples from both Finn and Hulk were cloned to determine the diversity of the Type II CBB Cycle. Pinpointing unique differences in gene distributions can provide clues to how these pathways originated and their overall prevalence in these systems.

Clones from each set of samples investigated were from hydrothermal chimneys found off the JdFR, originating from different vent fields. Phylogenetic trees were produced for both *cbbM* gene sequences and translated protein sequences. Upon examination of the both DNA and protein phylogenetic trees, it was shown that *cbbM* sequences vary amongst both chimney systems and throughout chimney gradients. Functional phylogeny has been shown to play a role in capturing deep lineages otherwise not captured through 16S rRNA phylogenetic surveys (Tourova, Kovaleva et al. 2010). This can be seen through examination of each cluster showing distinct groups of *Proteobacteria* amongst different ecosystem classifications. It appears that organism adaptations to hydrothermal ecosystems play a major role in the clustering of *cbbM* genes rather than overall phylogeny. Upon comparison of Finn and Hulk sequences, sequences were clustered apart even with distinct clusters among the same chimney environment.

The most diverse and secluded cluster was the “Mothra Vent Chimney” Community cluster. Throughout this cluster there were clones from both exterior and middle Finn chimney gradients. Grouped apart from the rest of the Finn sequences, this may represent a distinct clade within this specific chimney niche. The closest BLAST hits were magnetotactic

Gammaproteobacteria and *Alphaproteobacteria* from the Mothra hydrothermal vent field from a separate study (Xie, Wang et al. 2011).

It has been speculated that there could be groupings of bacteria specifically adapted to all vent environments. Through a comparative metagenomic study by Xie et al, they were able to show that very dissimilar vent environments harbor genes for unique physiological and functional adaptations. This could indicate the presence of specific clades of microorganisms indigenous to all vent environments (Xie, Wang et al. 2011). If this is the case, then one may be able attribute the similar diversity of the *cbbM* gene among different taxonomic groups to physical adaptations to exterior and middle chimney gradients. Formation of specific bacterial communities could be attributed to characteristic fluid mixing with at each hydrothermal locale.

Through the phylogenetic study of the *cbbM* gene it was shown to have great sequence diversity amongst both chimney ecosystems and gradients. *cbbM* diversity could stem from variations in sequence due to environmental confinement of this gene to distinct niches throughout the chimney wall. Clustering of diverse *cbbM* sequences could represent a distinct community of microorganisms physically adapted to vent ecosystems. Through the investigation of other hydrothermal ecosystems and the advent of comparative metagenomics, the elucidation of chimney-specific clades could be resolved in the future.

CHAPTER 6: CONCLUSION

INTRODUCTION

The goal of this thesis was to provide a linkage between microbial diversity and functional processes in hydrothermal chimney microorganisms. This was investigated by providing a baseline classification of microbial community diversity and linking this to the occurrence of the Calvin Benson-Bassham (CBB) pathway of carbon assimilation. There have been many microbial diversity studies performed at the hydrothermal chimneys in the past, but few linked microbial diversity to a functional basis. In addition, previous studies of the CBB cycle within hydrothermal systems have determined its presence in the symbiotic community around and upon vent chimneys (Nakagawa and Takai 2008). There has only been a few studies within the vent chimney that have examined its presence, mostly in the metagenomic realm examining environmental samples within the chimney walls (Wang, Zhou et al. 2009). Functional analyses in this thesis take a systematic approach to investigating the presence of the CBB cycle amongst various chimneys and throughout different gradients within.

MICROBIAL COMMUNITY STRUCTURE

Hydrothermal chimney ecosystems harbor very diverse microbial communities which have yet to be completely constrained. It is thought that a multitude of environmental, chemical and physical factors play a role in determining microbial community selection and dispersal (Schrenk, Holden et al. 2008). In this thesis, studies were aimed towards establishing what types of microbial communities were present within hydrothermal chimney ecosystems, their overall abundance throughout chimney gradients, and ecological influences determining their overall distribution.

In order to understand microbial community structure one must first understand the evolution and “life” of a vent chimney. There are three main stages of chimney development including: (1) venting and mineral precipitation, (2) chimney solidification and mineral maturation, and (3) inactivity marked after the cessation of venting. Each period is marked by diverse mineralogical and physical changes placing selective pressures upon overall community structure (Schrenk, Holden et al. 2008). Chimneys begin to develop with the vigorous mixing of hot hydrothermal fluids with cold seawater causing the precipitation of anhydrite and sulfide particles at temperatures of 150°C. Over time as temperature lowers and fluid mixing becomes less vigorous, lower temperature sulfide minerals form an edifice in which the chimney structure further solidifies. Contained within the edifice, is the central conduit that vents hydrothermal fluids lined with chalcopyrite. Conductive cooling towards the chimney exterior leads to the deposition of amorphous silica. As chimneys mature, their porous structure allows constant fluid-flow and mixing leading to the establishment of thermal and chemical gradients (Kelley, Baross et al. 2002). Once the flow of hydrothermal fluids cease, the chimney succumbs to weathering and overall fluid temperature drops to that of surrounding seawater (Tivey 1995).

During a chimney’s aging process, a plethora of microbial communities colonize and disperse amongst ecological niches throughout the chimney wall within its porous matrix (Schrenk, Kelley et al. 2003). Initial analyses in this thesis were conducted to help gain a sense of microbial community dispersal throughout the hydrothermal chimney environment. Through the use of taxonomic screens and community analyses amongst different chimney ecosystems, the presence and dispersal of Archaea and bacteria communities were further elucidated. Throughout Chapters II and III of this thesis analyses were conducted on incubators and

chimneys from both the Juan de Fuca Ridge and compared to studies of different hydrothermal chimney environments throughout the world.

The analyses in Chapter II were conducted on sulfides and incubators from the Main Endeavor Segment of the Juan de Fuca Ridge. These analyses aimed towards constraining the distribution and abundance of archaeal and bacterial communities originating from different chimneys and gradients found throughout this region. Biomass measurements in conjunction with taxonomic screens established that the most abundant microbial communities were found along middle-to-exterior chimney gradients, consistent with previous studies. Taxonomic gene abundance values indicated a steady microbial population of Archaea and Bacteria throughout chimneys and gradients with a higher abundance of Archaea than Bacteria in relation to gene abundance data. Community analyses by means of t-RFLP were conducted to further understand community diversity and dispersal throughout chimneys and their respective gradients. Species richness estimates first indicated that the most diverse microbial communities were found within middle chimney gradients for both the Archaea and Bacteria populations. Community similarity analyses were unable to pinpoint which factors controlled archaeal and bacterial community dispersal, but did suggest an overall environmental influence on the distribution of communities amongst different vent chimney gradients.

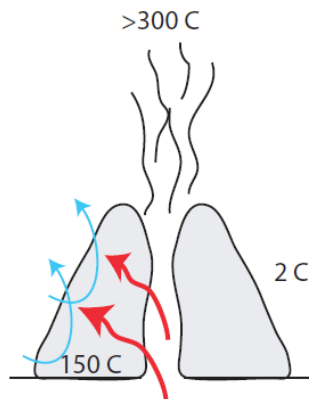
Slightly different from the community analyses in Chapter II, the analyses in Chapter III aimed towards gaining a larger picture on what archaeal and bacterial community dispersal looked like amongst vent fields worldwide. These analyses aimed towards gaining a more complete picture on linking ecological factors to community dispersal. The compilation of sequence data from multiple vent studies was used to create visual outputs allowing the pairing of ecological data to genomic data. Bacterial samples were clustered together based upon their

geography dependent on chimney origin. Key groupings included both natural chimneys and incubators sequences from the Southern Mariana Trough (SMT), the East Pacific Rise (EPR), and the Mothra field. Meanwhile, Archaea community dispersal seemed to be influenced by environmental factors with main clusters including exterior chimney gradients, long and short duration incubators, nascent chimneys, mature “white smoker” chimney environments, and inactive chimneys. Through pairing community analyses alongside vent mineralogy and evolution an overall schematic of microbial colonization in vent environments was composed in Figure 6-1.

Physical-chemical changes

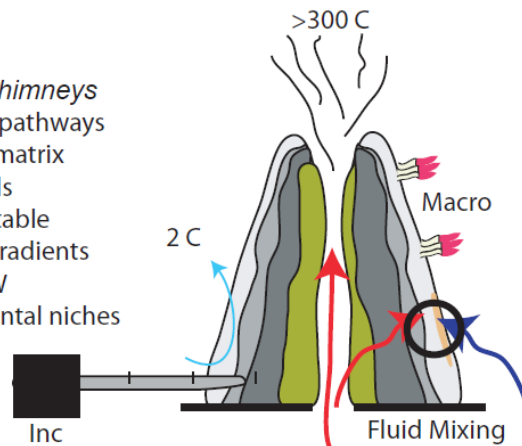
Stage I - Nascent Chimneys

- High temperatures (>150°C)
- High porosity
- Turbulent mixing of SW and HF's.
- Intermittent oxygen exposure
- Oxidation of Fe/S on surfaces?
- Pyrite precip., H₂ production
- Low organic carbon content
- clay?, anhydrite?



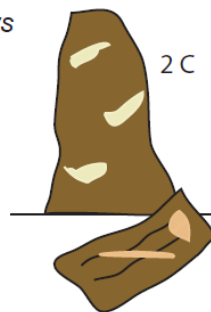
Stage II - Active Chimneys

- Restriction of flow pathways
- Infilling of porous matrix with sulfide minerals
- Establishment of stable thermal-chemical gradients between HF and SW
- Diverse environmental niches



Sulfide weathering - Mature Chimneys

- Hydrothermal flow wanes
- Low temperatures
- Seawater infiltration
- Oxidation of sulfide minerals
- Structural collapse



Microbiological changes

- Low microbial abundances
- Autotrophic metabolisms
- Ox/red of Fe and S compounds
- High abundance of deeply-branching uncultured Archaea

- High microbial abundances
- Diverse microbial metabolisms and physiologies
- Proteobacteria found throughout chimney environment
- Thermophilic bacteria (Epsilon) towards middle gradients
- Cultured Crenarchaeota found throughout
- Uncultured Crenarchaeota in high temp. interior regions
- Macrofaunal and microfaunal (Gamma) colonization of exterior surfaces

- Consumption of pre-formed organic material by heterotrophs
- Microbially-mediated metal sulfide oxidation
- Gammaproteobacteria and Crenarchaeota predominate

Figure 6-1: Model for vent evolution and subsequent microbial colonization

In this model it can be seen that there are specific hydrothermal chimney colonization trends for both Archaea and Bacteria. Archaea communities have two main types of colonizers, thermophilic-to-hyperthermophilic uncultured Crenarchaeota which colonize high temperature

nascent chimneys and vent interior gradients. Alternatively, there is culturable Marine Group I Crenarchaeota which thrives throughout chimney gradients mainly towards cooler exterior gradients. These organisms are found in mature and even inactive chimneys due to inherent pelagic adaptations to deep-sea environments (Madigan and Martinko 2006).

Bacterial colonization is limited to middle and exterior chimney gradients ranging from psychrophilic to thermophilic conditions. Thermophilic vent colonizers include, *Thermus* and *Aquificales* species which can withstand temperatures in up to 95°C (Madigan and Martinko 2006). Other bacteria colonizers are members of the *Proteobacteria* classification, and depending on the subgroup can inhabit a variety of niches within middle-to-exterior gradients especially *Epsilonproteobacteria*. The *Gammaproteobacteria* which are benthic in nature are restricted to exterior chimney gradients (Madigan and Martinko 2006).

FUNCTIONAL DIVERSITY OF VENT CHIMNEY INHABITANTS

Initial analyses in this thesis pieced together a picture of microbial diversity throughout vent chimney ecosystems. Further analyses in Chapters IV and V aimed towards understanding microbial carbon assimilation in hydrothermal vent chimneys and while providing a link to microbial diversity. The Type II Calvin Benson-Bassham Cycle (CBB) is one way microorganisms assimilate carbon in hydrothermal ecosystems (Nakagawa and Takai 2008). This study in particular utilized functional analyses to elucidate characteristic carbon and genomic signatures to determine the presence, abundance, and distribution of the CBB cycle in hydrothermal chimney ecosystems. This was performed through assaying for the *cbbM* gene throughout sulfide samples. This gene codes for the key regulatory enzyme in the Type II CBB cycle specifically prevalent in hydrothermal ecosystems (Nakagawa and Takai 2008).

In Chapter IV, analyses were conducted to determine the presence the CBB cycle throughout natural vent samples from the Endeavour Segment of the Juan de Fuca Ridge. Analyses were performed to look for specific carbon and genomic signatures of the CBB cycle amongst sulfide samples. Through both carbon isotopic analyses and genomic assays the presence of the CBB cycle was elucidated in hydrothermal chimney ecosystems. The *cbbM* gene was found throughout middle to exterior chimney gradients with its highest abundance in middle chimney gradients. Through comparison with taxonomic gene abundance data it was shown that *cbbM* corresponded to a significant proportion of the bacteria population.

Phylogenetic analyses of the *cbbM* gene performed in Chapter V of this thesis were used to observe the overall distribution of the *cbbM* gene throughout vent chimney populations. *cbbM*-positive clones were obtained from samples in the Mothra Vent Field located on the Main Endeavour Segment of the Juan de Fuca Ridge. These samples included natural sulfides from Finn, incubator samples from Hulk, and a background sample from the Main Endeavour Field. Phylogenetic trees were produced for both DNA and protein sequences. Both phylogenetic tree outputs showed the distribution of *cbbM* varying amongst both chimneys and throughout gradients. Clusters of *cbbM* sequences were diversified based upon distinct habitats within chimney ecosystems. Sub-groupings of *Proteobacteria* were clustered amongst different chimney habitats. A schematic of overall *cbbM* distribution in vent chimneys studied is shown below in Figure 6-2.

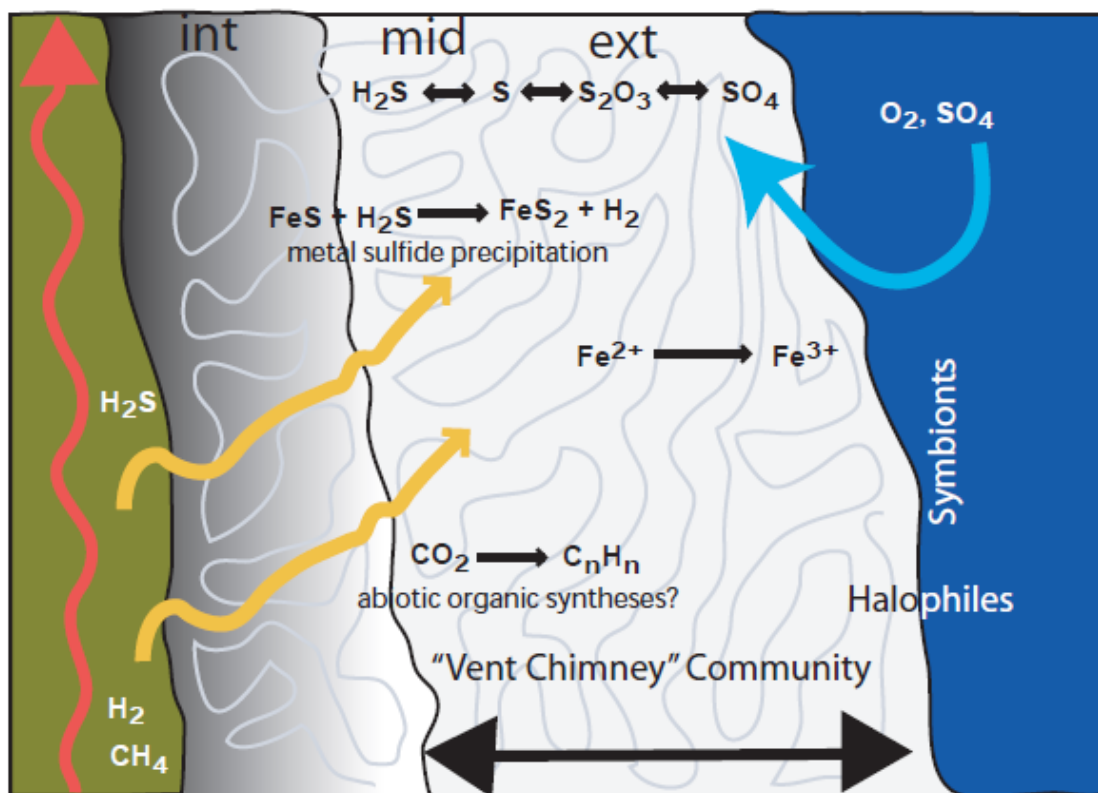


Figure 6-2: *cbbM* distribution amongst chimney habitats

Carbon assimilation throughout the vent chimney wall is fueled through the mixing of hot reduced hydrothermal fluids and cold oxygenated seawater. Mixing of these fluids throughout pore spaces of hydrothermal chimneys creates chemical disequilibrium culminating in a huge outpouring of free energy powering diverse energy utilization pathways. These pathways in turn have the potential to fuel chemolithoautotrophic metabolisms (McCollom and Shock 1997; Amend and Shock 2001). The highest extent of fluid mixing occurs within middle chimney gradients positioned in between end member fluids. The highest amount of energy is produced in this region fuelling biomass production and a diverse array of metabolisms. The CBB cycle is one such pathway that is fueled through this chemical disequilibrium.

As mentioned previously upon phylogenetic analysis, there proved to be diversity amongst *cbbM* harboring microbial communities throughout the hydrothermal chimney ecosystems. This diversity was found within the *Proteobacteria* classification. *Gammaproteobacteria* endosymbiont communities were found primarily towards vent exterior regions while *Epsilon*, *Alpha*, and *Betaproteobacteria* were found throughout middle and exterior chimney gradients. Functional resolution of the *Proteobacteria* community in chimneys can provide information leading towards elucidating specific set hydrothermal community amongst all hydrothermal chimney ecosystems.

FUTURE DIRECTIONS

This thesis has shown the presence of a diverse microbial population linked to biosignatures specific to the Type II Calvin Cycle within hydrothermal chimney ecosystems. Even though characteristic biosignatures have been found, active carbon assimilation by means of the Calvin Cycle has yet to be constrained throughout hydrothermal chimney walls. Future directions aim towards proving that the CBB pathway amongst other carbon assimilation pathways is present and actively occurring amongst microorganisms within the hydrothermal chimney niche. This can be performed through genetic and geochemical approaches.

Through the advent of new generation sequencing technologies, one can pinpoint the presence of multiple functional genes within hydrothermal chimney ecosystems (Wang, Zhou et al. 2009). Functional genes belonging to the same carbon assimilation within environmental samples can be pieced together providing more evidence for a pathway's presence. In addition, the expression of functional genes can be examined to determine which genes play direct roles in microbial carbon assimilation in vent environments.

Geochemical approaches can be paired alongside genomic methodologies through the use of stable isotope probing. Stable isotope probing measures the flow of stable carbon isotopes throughout an environmental system. This method can be used to constrain carbon assimilation in chimney ecosystems. Using this method, the flow of carbon can be traced to incorporation into microbial biomass. Through looking at isotope incorporation into DNA and performing genetic assays one can determine directly the means of carbon assimilation.

REFERENCES

- Amend, J. and E. Shock (2001). "Energetics of Overall Metabolic Reactions of Thermophilic and Hyperthermophilic Archaea and Bacteria." FEMS Microbial Review **25**(2): 175-243.
- Ashida, H., Y. Saito, et al. (2003). "A Functional Link Between RuBisCO-like Protein of Bacillus and Photosynthetic RuBisCO." Science **302**(5643): 286-290.
- Atomi, H. (2002). "Microbial Enzymes Involved in Carbon Dioxide Fixation." Journal of Bioscience and Engineering **94**(6): 497-505.
- Bach, W., K. Edwards, et al. (2006). "Energy in the Dark: Fuel for Life in the Deep Ocean and Beyond." EOS **87**(7): 73-78.
- Badger, M. R. and E. J. Bek (2008). "Multiple RuBisCO Forms in Proteobacteria: Their Functional Significance in Relation to CO₂ Acquisition by CBB Cycle." Journal of Experimental Botany **57**(7): 1525-1541.
- Berg, I. A., D. Kockelkorn, et al. (2010). "Autotrophic Carbon Fixation Pathways in Archaea." Nature Reviews Microbiology **14**(11): 488-496.
- Brazelton, W. J. and J. A. Baross (2009). "Abundant Transposases Encoded by the Metagenome of a Hydrothermal Chimney Biofilm." The ISME Journal **3**: 1420-1424.
- Brazelton, W. J., M. O. Schrenk, et al. (2006). "Methane- and Sulfur-Metabolizing Microbial Communities Dominate the Lost City Hydrothermal Field Ecosystem." Appl. and Environ. Microbiol. **72**(9): 6257-6270.
- Bryant, D. A. and N. U. Frigard (2006). "Prokaryotic Photosynthesis and Phototrophy Illuminated." Trends in Microbiology **14**(11): 488-496.
- Campbell, B. J., A. S. Engel, et al. (2006). "The Versatile ϵ -proteobacteria: Key Players in Sulphidic Habitats." Nature Reviews Microbiology **4**: 458-468.
- Cody, G. D., N. Z. Boctor, et al. (2004). "Assaying the Catalytic Potential of Transition Metal Sulfides for Abiotic Carbon Fixation." Geochimica et Cosmochimica Acta **68**(10): 2185-2196.
- Culman, S. W., R. Bukowski, et al. (2009). "T-REX: Software for the Processing and Analysis of T-RFLP data." BMC Bioinformatics **10**: 171.
- Delong, E. F. (1992). "Archaea in Coastal Marine Environments." PNAS **89**: 5685-5689.
- Deming, J. W. and J. A. Baross (1993). "Deep-sea Smokers: Windows to a Subsurface Biosphere?" Geochimica et Cosmochimica Acta **57**(14): 3219-3230.

- DeSantis, T. Z., P. Hugenholtz, et al. (2006). "Greengenes, a Chimera-Checked 16S rRNA Gene Database and Workbench Compatible with ARB." Appl. and Environ. Microbiol. **72**: 5069-5072.
- Eberhard, C., C. O. Wirsen, et al. (1995). "Oxidation of Polymetal Sulfides by Chemolithoautotrophic Bacteria from Deep-Sea Hydrothermal Vents." Geomicrobiology Journal **13**(3): 145-164.
- Edwards, K., P. L. Bond, et al. (2000). "An Archaeal Iron-Oxidizing Extreme Acidophile Important in Acid Mine Drainage." Science **287**: 1796-1799.
- Elsaied, H. and T. Naganuma (2001). "Phylogenetic Diversity of Ribulose-1, 5-Bisphosphate Carboxylase/Oxygenase Large-Subunit Genes from Deep-Sea Microorganisms" Appl. and Environ. Microbiol. **67**(4): 1751-1765.
- Fierer, N., J. A. Jackson, et al. (2005). "Assessment of Soil Microbial Community Structure by use of Taxon-Specific Quantitative PCR Assays." Appl. and Environ. Microbiol. **71**(7): 4117-4120.
- Goury, M., S. Guindon, et al. (2010). "Seaview Version 4: a Multiplatform Graphical User Interface for Sequence Alignment and Phylogenetic Tree Building." Molecular Biology and Evolution **27**(2): 221-224.
- Hall, J. R., K. R. Mitchell, et al. (2008). "Molecular Characterization of the Diversity and Distribution of a Thermal Spring Microbial Community by Using rRNA and Metabolic Genes." Appl. and Environ. Microbiol. **75**(15): 4910-4922.
- House, C. H., W. J. Schopf, et al. (2003). "Carbon Isotopic Fractionation by Archaeans and Other Thermophilic Prokaryotes." Organic Geochemistry **34**: 345-356.
- Huber, J. A., D. B. M. Welch, et al. (2007). "Microbial Population Structures in the Deep Marine Biosphere." Science **318**(97): 97-100.
- Hugler, M., H. Huber, et al. (2003). "Autotrophic CO₂ Fixation Pathways in Archaea (Crenarchaeota)." Arch. Microbiol. **179**: 160-173.
- Jannasch, H. W. (1985). "Geomicrobiology of Deep-Sea Hydrothermal Vents." Science **229**(4715): 717-725.
- Jordan, D. B. and W. L. Ogren (1983). "Species Variation in Kinetic Properties of Ribulose 1-5-Bisphosphate Carboxylase/ Oxygenase." Archives of Biochemistry and Biophysics **227**(2): 425-433.
- Kato, S., Y. Takano, et al. (2010). "Biogeography and Biodiversity in Sulfide Structures of Active and Inactive Vents at Deep-Sea Hydrothermal Fields of the Southern Mariana Trough." Appl. and Environ. Microbiol. **76**(9): 2968-2979.

- Kelley, D. S. (2010). The Deep, Hot Biosphere: What are the Maximum Temperatures Life Can Survive? Adobe. Ridge2010Postersm.
- Kelley, D. S., J. A. Baross, et al. (2002). "Volcanoes, Fluids, and Life at Mid-Ocean Ridge Spreading Centers." Annual Review of Earth and Planetary Sciences **30**: 385-491.
- Kelley, D. S., J. R. Delaney, et al. (2001). "Geology and Venting Characteristics of the Mothra Hydrothermal Field, Endeavour Segment, Juan de Fuca Ridge." Geology **29**(10): 959-962.
- Kristall, B., D. S. Kelley, et al. (2006). "Growth History of a Diffuse Venting Sulfide Structure from the Juan de Fuca Ridge: A Petrological and Geochemical Study." American Geophysical Union **7**(Geochemistry Geophysics Geosystems).
- Lang, S. Q., D. A. Butterfield, et al. (2006). "Dissolved Organic Carbon in Ridge-axis and Ridge-flank Hydrothermal Systems." Geochimica et Cosmochimica Acta **70**(15): 3830-3842.
- Madigan, M. T. and J. M. Martinko, Eds. (2006). Prokaryotic Diversity. Brock Biology of Microorganisms. Upper Saddle River, NJ.
- McCarthy, M. D., S. R. Beaupre, et al. (2011). "Chemosynthetic Origin of ¹⁴C-depleted Dissolved Organic Matter in a Ridge-flank Hydrothermal System." Nature Geoscience **4**: 32-36.
- McCliment, E. A., K. M. Voglesonger, et al. (2006). "Colonization of Nascent Deep-sea Hydrothermal Vents by a Novel Archaeal and Nanoarchaeal Assemblage." Environ Microbiol **8**(1): 114-125.
- McCollom, T. M. and E. L. Shock (1997). "Geochemical Constraints on Chemolithoautotrophic Metabolism by Microorganisms in Seafloor Hydrothermal Systems." Geochimica et Cosmochimica Acta **61**: 4375-4391.
- McCollom, T. M. (2008). "Magma-to-Microbe Networks in the Context of Sulfide Hosted Microbial Ecosystems." American Geophysical Union: 193-213
- Nakagawa, S. and K. Takai (2008). "Deep Sea Vent Chemotrophs: Diversity, Biochemistry, and Ecological Significance." FEMS **65**: 1-14.
- O'Leary, M. H. (1988). "Carbon Isotopes in Photosynthesis." Bioscience **38**(5): 328-336.
- Reysenbach, A.-L., K. Longnecker, et al. (2000). "Novel Bacterial and Archaeal Lineages from an In Situ Growth Chamber Deployed at a Mid-Atlantic Ridge Hydrothermal Vent." Appl. and Environ. Microbiol. **66**(9): 3789-3806.

- Schloss, P. D., S. L. Westcott, et al. (2009). "Introducing Mothur: Open-Source, Platform-Independent, Community-Supported Software for Describing and Comparing Microbial Communities." Appl. and Environ. Microbiol. **75**(23): 7537-7541.
- Schrenk, M. O., J. F. Holden, et al. (2008). "Magma-to-Microbe Networks in the Context of Sulfide Hosted Microbial Ecosystems." American Geophysical Union: 233-258.
- Schrenk, M. O., D. S. Kelley, et al. (2003). "Incidence and Diversity of Microorganisms within the Walls of an Active Deep-sea Sulfide Chimney." Appl. and Environ. Microbiol. **69**(6): 3580-3592.
- Takai, K., T. Komatsu, et al. (2001). "Distribution of Archaea in a Black Smoker Chimney Structure." Appl. and Environ. Microbiol. **67**(8): 3618-3629.
- Thauer, R. K. (2007). "A Fifth Pathway of Carbon Fixation." Science **318**: 1732-1733.
- Tivey, M. K. (1995). "Modeling Chimney Growth and Associated Fluid Flow at Seafloor Hydrothermal Vent Sites." American Geophysical Union **91**: 158.
- Tivey, M. K., S. E. Humphris, et al. (1995). "Deducing Patterns of Fluid Flow and Mixing within the TAG Active Hydrothermal Mound using Mineralogical and Geochemical Data." Journal of Geophysical Research **100**(B7): 527-555.
- Tourova, T. P., O. L. Kovaleva, et al. (2010). "Ribulose-1, 5-bisphosphate Carboxylase/Oxygenase Genes as a Functional Marker for Chemolithoautotrophic Halophilic Sulfur-Oxidizing Bacteria in Hypersaline Habitats." Microbiology **156**: 2016-2025.
- Ver Eecke, H. C., D. S. Kelley, et al. (2009). "Abundances of Hyperthermophilic Fe (III) Oxide Reducers and Heterotrophs in Hydrothermal Sulfide Chimneys of the Northeastern Pacific Ocean." Appl. and Environ. Microbiol. **75**(1): 242-245.
- Wang, F., H. Zhou, et al. (2009). "GeoChip-based Analysis of Metabolic Diversity of Microbial Communities at the Juan de Fuca Ridge Hydrothermal Vent." PNAS **106**(12): 4840-4845.
- Weisburg, W. G., S. M. Barnes, et al. (1991). "16S Ribosomal DNA Amplification for Phylogenetic Study." Journal of Bacteriology **173**(2): 697-703.
- Xie, W., F. Wang, et al. (2011). "Comparative Metagenomics of Microbial Communities Inhabiting Deep-sea Hydrothermal Vent Chimneys with Contrasting Chemistries." The ISME Journal **5**: 2011.